these diseases. Neuropathologically, α-synuclein lesions are believed to spread progressively throughout the brain and their spread correlates to the staging of clinical symptoms (Muller *et al.*, 2005), as in the case of tau pathology in Alzheimer's disease (Braak and Braak, 1991). Kordower *et al.* (2008) and Li *et al.* (2008) reported that embryonic neurons transplanted into the striatum of an individual with Parkinson's disease developed Lewy body-like pathologies, suggesting that pathological α-synuclein may be transmissible from diseased neurons to healthy neurons. Recent studies have also shown that exogenous α-synuclein fibrils induced Lewy body pathology in cultured neurons (Desplats *et al.*, 2009; Emmanouilidou *et al.*, 2010; Nonaka *et al.*, 2010; Volpicelli-Daley *et al.*, 2011), transgenic mouse brain (Mougenot *et al.*, 2012; Luk *et al.*, 2012*b*) and wild-type mouse brain (Luk *et al.*, 2012*a*). In addition, a growing body of evidence indicates that self-propagating protein aggregates play central roles in many neurodegenerative diseases, including Parkinson's disease and Alzheimer's disease (Clavaguera *et al.*, 2009; Mougenot *et al.*, 2012; Luk *et al.*, 2012*b*; Stohr *et al.*, 2012). In this work, we have tested whether inoculation of insoluble α-synuclein from brains with dementia with Lewy bodies and synthetic mouse and human α-synuclein fibrils can induce α-synuclein pathology in wild-type mice. As a result, we have established a new mouse model of sporadic α-synucleinopathy using wild-type mice.

Materials and methods

Preparation of recombinant α-synuclein monomer and fibrils

Human and mouse α-synuclein were expressed in *E. coli* BL21 (DE3) cells, as described (Masuda *et al.*, 2006*b*). To avoid the production of α-synuclein dimers induced by misexpression of cysteine-containing α-synuclein, the Y136-TAT construct was used (Masuda *et al.*, 2006*a*). α-Synuclein was purified by boiling, Q-Sepharose® ion exchange chromatography and ammonium sulphate precipitation, before dialysis against 30 mM Tris–HCl, pH 7.5. Recombinant proteins were centrifuged at 113 000*g* for 20 min at 4°C to remove insoluble materials and used as α-synuclein monomer. Protein concentrations were determined as described (Yonetani *et al.*, 2009). Purified human and mouse α-synuclein (7 mg/ml) were incubated at 37°C in a shaking incubator (200 rpm) in 30 mM Tris–HCl, pH 7.5, containing 0.1% NaN_3, for 72 h. α-Synuclein fibrils were pelleted by spinning the assembly mixtures at 113 000*g* for 20 min.

Preparation of the insoluble fraction of dementia with Lewy bodies brain

Fresh frozen brain tissue from a patient with dementia with Lewy bodies (phosphorylated α-synuclein pathology is shown in Supplementary Fig. 9) was homogenized in 18 volumes (w/v) of Buffer A (10 mM Tris-HCl, pH 7.4, 0.8 M NaCl, 1 mM EGTA, and 10% sucrose), and sarkosyl was added to the homogenate at a concentration of 2%. The mixture was incubated for 30 min at 37°C, sonicated and spun at 9100*g* for 10 min at 25°C. The supernatant was further centrifuged at 113 000*g* for 20 min at 25°C, and the sarkosyl-insoluble pellet was washed with Buffer A. The pellet was taken up in saline, sonicated and centrifuged at 800*g* for 5 min. The supernatant was used for stereotaxic injection.

Stereotaxic surgery

Four- to six-month-old female C57BL/6J mice (CLEA Japan, Inc.) anaesthetized with 50 mg/kg pentobarbital sodium were injected with 10 μg of recombinant α-synuclein monomer, fibrils or 5 μl of insoluble fraction of dementia with Lewy bodies brain into substantia nigra (anterior-posterior: −3.0 mm; medial-lateral: −1.3 mm; dorsal-ventral: −4.7 mm from the bregma and dura) using a 10-μl Hamilton syringe. Mice were anaesthetized with isoflurane and killed by decapitation. For immunohistochemistry, brains were fixed in 10% formalin neutral buffer solution (Wako), and for biochemical analysis, brains were snap-frozen on dry ice and stored at −80°C. All experimental protocols were approved by the Animal Care and Use Committee of the Tokyo Metropolitan Institute of Medical Science.

Immunohistochemistry

Brains fixed in 10% formalin were cut on a vibratome (Leica) at 50 μm thickness. The free-floating sections were treated with 0.5% H_2O_2 in methanol for 30 min to inactivate peroxidase and blocked with 10% calf serum in PBS. Sections were immunostained with appropriate antibodies. Antibodies used in this study are summarized in Supplementary Table 1. After incubation with the biotinylated-secondary antibody (Vector), labelling was detected using the ABC staining kit (Vector).

Confocal microscopy

For double-label immunofluorescence for phosphorylated α-synuclein and ubiquitin or phosphorylated α-synuclein and p62, brain sections were incubated overnight at 4°C in a cocktail of 1175 and anti-ubiquitin or anti-p62 antibody. The sections were then washed and incubated in a cocktail of Alexa Fluor® 568-conjugated goat anti mouse IgG (Molecular Probes) and Alexa Fluor® 488-conjugated goat anti mouse IgG (Molecular Probes). After further washing, sections were stained with TO-PRO®-3, coverslipped with VECTASHIELD® (Vector) and observed with a laser-scanning confocal fluorescence microscope (LSM5 PASCAL, Carl Zeiss).

Biochemical analysis

Mouse brains were homogenized in 20 volumes (w/v) of Buffer A, then spun at 100 000*g* for 30 min at 4°C, and the supernatant was retained as buffer-soluble fraction. The pellet was homogenized in 20 volumes of Buffer A containing 1% Triton™ X-100 and incubated for 30 min at 37°C. After centrifugation at 100 000*g*, the Triton™-insoluble pellet was further homogenized in Buffer A containing 1% sarkosyl and incubated at 37°C for 30 min. Samples were spun at 100 000*g* for 30 min. The sarkosyl-pellet was sonicated in 30 mM Tris-HCl, pH 7.4, and used for immunoblotting as sarkosyl-insoluble fraction. The samples were subjected to SDS-PAGE on 12.5% polyacrylamide gel and proteins were electrotransferred onto a polyvinylidene difluoride membrane, probed with appropriate antibodies and detected as described (Nonaka *et al.*, 2009).

Behavioural tests

Open field test

Each mouse was placed in the centre of the open field apparatus (25-cm diameter). Activity was measured by SUPERMEX system (Muromachi Kikai) over 90-min period and analysed by CompACT AMS software ver.3 (Muromachi Kikai). Total activity was measured by counting the number of photobeam interruptions over every 5-min period.

Wire hang test

Neuromuscular strength was tested with a wire hang test. The mouse was placed on a wire mesh, waved gently so that the mouse gripped the wire and then inverted. Latency to fall was recorded with a 300-s cut-off time.

Rotarod test

The Rotarod test, using an accelerating Rotarod (Muromachi Kikai), was performed by placing mice on 9-cm diameter rods and measuring the time each animal was able to maintain its balance on the rod. We used 9-cm rods to make the test more sensitive to motor skill learning (Shiotsuki *et al.*, 2010). The speed of the rotarod accelerated from 0 to 40 rpm over a 5-min period.

Y-maze test

Y-maze apparatus (Muromachi Kikai) consisted of three arms (40 cm × 3 cm) made of grey plastic joined in the middle to form a Y shape. Mice were placed into one of the arms of the maze and allowed to explore freely the maze for an 8-min session. The alternation between arms was recorded.

Intranasal administration of abnormal α-synuclein fibrils

Twenty micrograms of recombinant α-synuclein monomer or preformed fibrils, or 10 μl of insoluble fraction of dementia with Lewy bodies brain, was administered intranasally once a week for 1 month to 10-week-old female C57BL/6J mice (soluble mouse α-synuclein, soluble human α-synuclein, mouse α-synuclein fibrils, human α-synuclein fibrils and dementia with Lewy bodies extracts, $n = 5$ per group). At 21 months after the last administration, mice were anaesthetized with pentobarbital sodium and killed by perfusion with phosphate buffer (pH 7.4) and 4% paraformaldehyde in 0.1% phosphate buffer. Brains were cryosectioned and immunostained as described above.

Results

To investigate whether insoluble α-synuclein fibrils can propagate *in vivo*, we injected recombinant human α-synuclein fibrils into the substantia nigra in the right cerebral hemisphere of C57BL/6J mice. α-Synuclein fibrils were prepared using highly purified recombinant α-synuclein (Supplementary Fig. 1A) by incubation with shaking. Formation of the fibrils was confirmed by electron microscopy (Supplementary Fig. 1B) and thioflavin S assay (data not shown). The fibrils were then collected by ultracentrifugation, sonicated and used for injection. Abnormal phosphorylated α-synuclein-positive structures were observed in the brains of mice injected with human α-synuclein fibrils at 15 months after inoculation (Fig. 1). Phosphorylated α-synuclein pathology was distributed throughout the brain including substantia nigra, amygdala, dentate gyrus, hippocampal CA1-3, molecular layer of hippocampus, fimbria, stria terminalis, hypothalamus, somatosensory area, visual cortex, cingulate cortex and corpus callosum (Fig. 1). Phosphorylated α-synuclein-positive structures were also positive for anti-ubiquitin and p62 antibodies (Fig. 2A). Co-localization was confirmed by confocal microscopy (Fig. 2B and C), indicating that these structures have the same immunoreactive properties as Lewy bodies (Kuusisto *et al.*, 2001). By contrast, no phosphorylated α-synuclein, ubiquitin or p62-positive pathology was observed in the brains of mice injected with soluble human α-synuclein (Supplementary Fig. 2). Remarkably, despite the unilateral injection of α-synuclein fibrils, phosphorylated α-synuclein-positive pathology appeared bilaterally (Fig. 3A). In the right hemisphere (injected side), phosphorylated α-synuclein pathology was seen abundantly in dentate gyrus and amygdala, whereas in the left hemisphere no pathology was seen in amygdala and only sparsely in dentate gyrus (Fig. 3A). These results strongly suggest that α-synuclein pathology propagates throughout the brain from the injection site. To understand the spreading pathway of phosphorylated α-synuclein pathology, we investigated in detail the distribution in four coronal sections at 15 months after inoculation (Fig. 3B). Near the injection level (bregma −3.40 mm), abundant phosphorylated α-synuclein pathology was present in substantia nigra, hippocampus, external capsule and entorhinal cortex in right hemisphere, whereas in the left hemisphere, sparser pathology was detected in hippocampus and external capsule (Fig. 3B). By contrast, at the level of 0.02 mm from bregma (3 mm anterior to the injection level), phosphorylated α-synuclein pathology was concentrated in stria terminalis, septal nucleus and cingulate, motor and somatosensory cortex in the right hemisphere. In the left hemisphere, phosphorylated α-synuclein pathology was detected only in septal nucleus (Fig. 3B). These results suggest that phosphorylated α-synuclein pathology does not spread by simple diffusion and the propensity to accumulate phosphorylated α-synuclein seems to differ among brain regions. The time course of spreading of phosphorylated α-synuclein pathology was analysed by immunohistochemistry and summarized in Table 1. Table 1 clearly indicates that induction of phosphorylated α-synuclein pathology in wild-type mice is time- and brain region-dependent. No signs of astrogliosis and inflammation were observed in human α-synuclein fibril-injected mice compared with soluble-human α-synuclein-injected mice at 15 months after injection (Supplementary Fig. 3).

To clarify which α-synuclein species accumulated in the mice, and when, we performed immunoblot analysis with LB509 and anti-mouse synuclein antibodies, which specifically recognize human α-synuclein and mouse α-synuclein, respectively. The antibody specificities are shown in Supplementary Fig. 1B. At a few

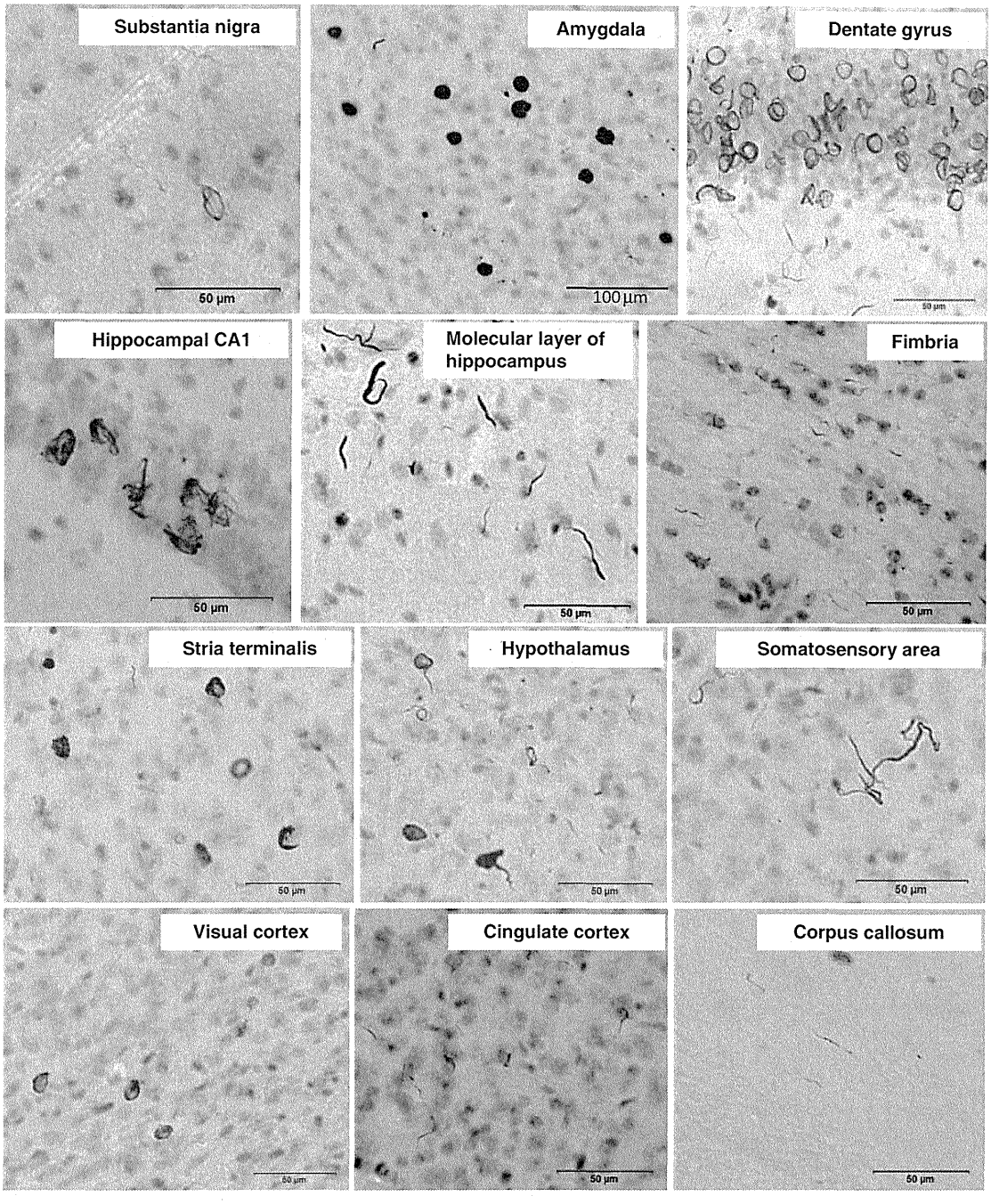

Figure 1 Induction of phosphorylated α-synuclein pathology in wild-type mouse brain injected with human α-synuclein fibrils, observed at 15 months after injection. Sections were immunostained with anti-phosphorylated α-synuclein antibody, 1175. The shapes of phosphorylated α-synuclein-positive structures differed among brain areas. Ring-like and Lewy neurite-like structures were observed in substantia nigra, hippocampus, hypothalamus, somatosensory area, visual cortex, cingulate cortex and corpus callosum, whereas Lewy body- and Lewy neurite-like structures were observed in amygdala and stria terminalis.

hours after injection (Day 0), injected recombinant human α-synuclein fibrils were detected in the sarkosyl-insoluble fraction of the right and left hemispheres by LB509 antibody, suggesting that injected human α-synuclein fibrils in the extracellular space spread quickly throughout the brain. However, at 7 days after injection, the human α-synuclein immunoreactivities had disappeared, and did not reappear at 30 or 90 days after injection (Fig. 4). At 90 days after injection, anti-phosphorylated α-synuclein-positive 15, 20, 30 and 35 kDa bands were detected in the sarkosyl-insoluble fractions. This band pattern is indistinguishable from that of pathological α-synuclein in dementia with Lewy bodies brain (Fig. 4). The 15, 20, 30 and 35 kDa bands correspond to α-synuclein monomer, mono-ubiquitinated α-synuclein, dimer and ubiquitinated dimer, respectively. Most

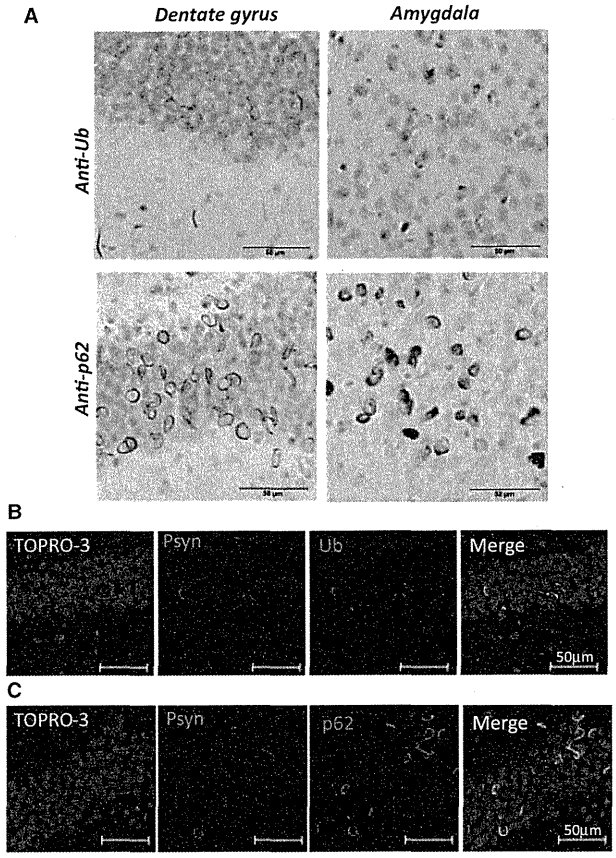

Figure 2 α-Synuclein pathology in fibril-injected mice brain was immunoreactive for ubiquitin (Ub) and p62. (**A**) Staining of dentate gyrus and amygdala of fibril-injected mice at 15 months after injection, using anti-ubiquitin (*upper*) and p62 (*lower*) antibodies. Abundant ubiquitin- and p62-positive pathology can be seen. (**B** and **C**) Double-labelled immunofluorescence of dentate gyrus for phosphorylated α-synuclein (Psyn) and ubiquitin (**B**) or p62 (**C**). Phosphorylated α-synuclein-positive structures were co-localized with ubiquitin and p62.

interestingly, anti-mouse α-synuclein strongly labelled the sarkosyl-insoluble phosphorylated α-synuclein-positive bands at Day 90, but these were not immunostained with LB509. These results clearly show that endogenous mouse α-synuclein is accumulated as phosphorylated and ubiquitinated forms. Immunohistochemical analysis with anti-tyrosine hydroxylase suggested that dopaminergic neurons are retained in substantia nigra of human α-synuclein fibril-injected mice at 6 months after injection (Fig. 5A and B). However, dramatic loss of the neurotransmitter enkephalin was observed in globus pallidus and amygdala central nucleus, where abundant phosphorylated α-synuclein-positive structures are detected (Fig. 5C and D). These data suggest that neuronal dysfunction occurs without apparent neuronal loss. We also performed behavioural analyses of mice injected with soluble human α-synuclein monomers or human α-synuclein fibrils. However, significant differences were not observed in open field test, wire hang test, rotarod test and Y-maze test (Supplementary Fig. 4) at 6 months after injection.

Next, we tested whether fibrils composed of recombinant mouse α-synuclein can induce α-synuclein pathology more efficiently than those composed of human α-synuclein, because the sequences of human and mouse α-synuclein are slightly different (Supplementary Fig. 5), and there could be a species difference. Mouse α-synuclein complementary DNA was cloned, and the protein was expressed in *Escherichia coli* and purified. Fibrils or soluble mouse α-synuclein were inoculated into substantia nigra of wild-type mouse brains and the pathology was evaluated. Strikingly, all the mice injected with mouse α-synuclein fibrils developed phosphorylated α-synuclein pathology in the injected side of the brain, whereas no pathology was detected in mice injected with soluble mouse α-synuclein (Table 2). The phosphorylated α-synuclein pathologies were basically the same as those of mice injected with human α-synuclein fibrils (data not shown). The efficiency of the induction of phosphorylated α-synuclein pathology by human α-synuclein fibrils was ~90% (Table 2), which is quite high, but slightly lower than that with mouse α-synuclein fibrils, suggesting that there may be a small species difference between mouse and human α-synuclein.

Finally, we tested whether pathological α-synuclein deposited in the brains of patients has similar prion-like properties in brains of wild-type mice. Surprisingly, pathological α-synuclein-enriched fractions also induced phosphorylated α-synuclein-positive pathologies in various areas of brain, including the substantia nigra, amygdala, hippocampus, striatum, hypothalamus, somatosensory area, motor cortex, piriform cortex and superior colliculus (Fig. 6). In brains of these mice, the phosphorylated α-synuclein-positive pathologies mostly resembled Lewy neurite-like structures. Lewy body-like pathology was detected only in amygdala and piriform cortex. The percentage of mice that developed phosphorylated α-synuclein pathology in the injected side of the brains was 50% in the group injected with insoluble phosphorylated α-synuclein of dementia with Lewy bodies brains, which is less than that in mice injected with recombinant α-synuclein fibrils (Table 2). Thus, these results demonstrate that inoculation of either pure synthetic recombinant α-synuclein fibrils or dementia with Lewy bodies brain extracts into wild-type mice can induce Lewy body/neurite-like phosphorylated α-synuclein pathology efficiently and reproducibly. Our results raise an important question, i.e. whether or not α-synuclein fibrils are transmissible among individuals. To test this possibility, we intranasally administered at high concentrarion of abnormal α-synuclein fibrils (preformed recombinant human or mouse α-synuclein fibrils) or the insoluble fraction from dementia with Lewy bodies brain to normal mice. However, no pS129-positive abnormal structures were detected in the brain at 21 months after the final administration (Supplementary Fig. 6), even with highly sensitive immunohistochemical staining, suggesting that the abnormal α-synuclein cannot pass through the nasal mucosa.

Discussion

In this study, we have shown that the inoculation of α-synuclein fibrils made of recombinant α-synuclein or dementia with Lewy bodies brain extracts into wild-type mouse brain is sufficient to

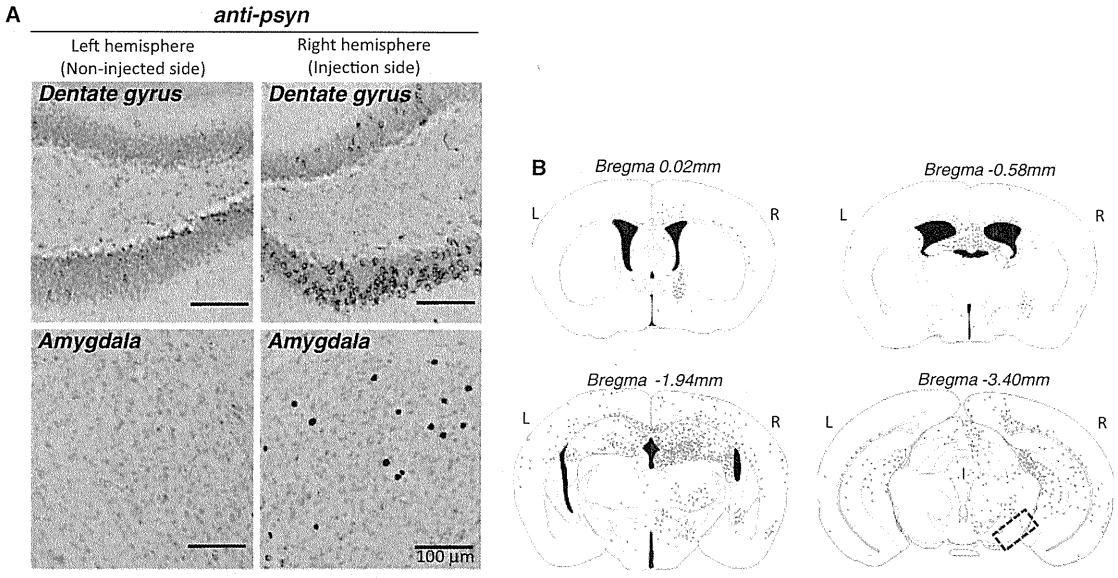

Figure 3 (**A**) Spreading of phosphorylated α-synuclein pathology on the contralateral side of mouse brain injected with α-synuclein fibrils. Staining of dentate gyrus and amygdala in the right hemisphere (injection side) and in the left hemisphere (non-injected side) with anti-phosphorylated α-synuclein (psyn) antibody, 1175, at 15 months after injection. (**B**) Distribution of phosphorylated α-synuclein pathology in human α-synuclein fibril-injected mouse brain at 15 months after injection ($n = 24$). Four coronal sections were stained with phosphorylated α-synuclein antibody, 1175. Red dots indicates Lewy bodies- and Lewy neurites-like pathology. Near the injection level (bregma -3.40 mm), abundant phosphorylated α-synuclein pathology was present in substantia nigra, hippocampus, external capsule, and entorhinal cortex in right hemisphere, whereas in the left hemisphere, sparser pathology was detected in hippocampus and external capsule. At the level of -1.94 mm from bregma, severe phosphorylated α-synuclein pathology was present in hippocampus, amygdala, corpus callosum, hypothalamus and motor, visual, somatosensory, auditory and piriform cortex in the right hemisphere, whereas moderate phosphorylated α-synuclein pathology was observed in corpus callosum, hippocampus, external capsule and motor, somasosensory and auditory cortex in the left hemisphere. At the level of -0.58 mm from bregma, phosphorylated α-synuclein pathology was detected in amygdala, corpus callosum, fimbria, fornix, hypothalamus, striatum and somatosensory and piriform cortex in the right hemisphere, whereas in the left hemisphere, the pathology was present in corpus callosum, fimbria, fornix, hypothalamus and striatum. At the level of 0.02 mm from bregma, phosphorylated α-synuclein pathology was concentrated in stria terminalis, septal nucleus and cingulate, motor and somatosensory cortex in the right hemisphere. In the left hemisphere, phosphorylated α-synuclein pathology was detected only in septal nucleus. Dashed box indicates substantia nigra (injection site). L = left hemisphere of brain; R = right hemisphere.

cause the appearance of Lewy body/neurite-like α-synuclein pathology *in vivo*. Similar work was recently published by Luk *et al.* (2012*a*) but there are important differences between our study and theirs. Luk *et al.* (2012*a*) showed that only inoculation of synthetic mouse α-synuclein fibrils into wild-type mouse brain induced synuclein pathology. In our present study, we inoculated not only fibrils made of recombinant mouse α-synuclein but also ones from human α-synuclein fibrils, and importantly also insoluble α-synuclein from dementia with Lewy bodies brains, into wild-type mouse brain. This is the first report showing efficient induction of α-synuclein pathology by inoculation of material from human brain. Furthermore, our biochemical analyses clearly demonstrate that endogenous mouse α-synuclein is converted into abnormal form and deposited in neurons of the brain through a prion-like mechanism or by seed-dependent aggregation by crossing the species barrier (Fig. 4). Since soluble α-synuclein never induced such pathology (Supplementary Fig. 2), we can conclude that the structural difference between soluble and filamentous forms of α-synuclein, i.e. cross-β structure in the α-synuclein fibrils (Serpell *et al.*, 2000) is critical for the pathogenesis. It has been reported that recombinant α-synuclein fibrils enhance the initiation and progression of α-synuclein pathology in transgenic mice overexpressing mutant α-synuclein (Mougenot *et al.*, 2012; Luk *et al.*, 2012*b*) and wild-type mice (Luk *et al.*, 2012*a*). In those models, α-synuclein pathology appeared at 90 days after inoculation. In our mouse model, abnormal phosphorylated α-synuclein pathology was also detected at 90 days after injection (Fig. 4 and Table 1), suggesting that it takes about this length of time for the formation of abnormal phosphorylated α-synuclein pathology *in vivo* after the seeding procedure. Despite a diffusion of injected exogenous α-synuclein fibrils to the bilateral sides of brain within a few hours after injection (Fig. 4), phosphorylated α-synuclein pathology seems to be initiated in the injected side and to spread from the injected side to the non-injected side in a time-dependent manner (Table 1). Thus, it is reasonable to speculate that exogenous fibrils enter neurons at the injection site as a result of infusion pressure, a temporary high concentration, or some other mechanism, and then the pathological process starts to develop from these cells.

Propagation patterns of pathology in the inoculated mice were basically identical regardless of the species of injected seeds (i.e. recombinant human α-synuclein fibrils, mouse α-synuclein fibrils or

Table 1 Semi-quantitative grading of α-synuclein pathology in mice injected with human α-synuclein fibrils

			Non-injection side (left hemisphere)			Injection side (right hemisphere)		
			Time from injection (days)			Time from injection (days)		
			90	180	450	90	180	450
Bregma	0.02 mm	Stria terminalis	–	–	–	–	+ +	+ + +
		Striatum	–	+	+	+	+ +	+ +
		Cigular cortex	–	–	–	–	+	+
		Septal nucleus	–	–	–	–	+	+
Bregma	−0.58 mm	Corpus callosum	–	–	+	–	–	+ +
		Fornix	–	+	+ +	–	+	+ +
		Hippocampal commissure	–	+	+ +	–	+	+ +
		Amygdala	–	–	–	+	+ + +	+ + +
		Globus pallidus	–	+	+	–	+	+ +
		Striatum	–	–	+	+	+	+
		Somatosensory area	–	–	+	–	+	+
		Insular cortex	–	–	–	+	+	+
Bregma	−1.94 mm	Corpus callosum	–	–	+ +	–	–	+ +
		Hippocampus	–	+	+ + +	+	+ +	+ + +
		Habenular nucleus	–	–	+	–	–	+ + +
		Fimbria	–	+	+ + +	–	+	+ + +
		Amygdala	–	–	–	+ +	+ + +	+ + +
		Hypothalamus	–	–	+	+	+	+ +
		Thalamus	–	–	–	–	–	+
		Visual cortex	–	–	+	–	+	+ +
		Somatosensory area	–	+	+	–	+	+ +
		Auditory cortex	–	–	+	+	+	+ +
		Piriform cortex	–	–	+	+	+	+ +
		External cupsule	–	–	+	–	–	+ +
Bregma	−3.40 mm	Substantia nigra	–	–	–	+	+	+
		Hippocampus	–	+	+ +	+	+ +	+ +
		Superior colliculus	–	+	+	–	+	+ +
		External cupsule	–	–	+	–	–	+
		Visual cortex	–	–	–	+	+	+
		Auditory cortex	+	+	+	+	+ +	+ +
		Entorhinal cortex	–	+	+	+	+ +	+ +

Four coronal sections were stained with anti-phosphorylated α-synuclein antibody at 90, 180 or 450 days after injection. Grading of α-synuclein pathology was performed as follows: –, none; +, slight; + +, moderate; + + +, severe. At 90 days after injection, small amounts of phosphorylated α-synuclein-positive structures were observed in substantia nigra, amygdala, striatum, hypothalamus, hippocampus, and stria terminalis in the right hemisphere of brain (injected side), but very few Lewy neurites were detected in cortex in the left hemisphere. At 180 days post-injection, the amount of phosphorylated α-synuclein-positive pathology was increased and was more widely spread in the right hemisphere, while in the left hemisphere, little phosphorylated α-synuclein pathology was apparent in hypothalamus, hippocampus, striatum or globus pallidus. At 450 days (15 months) after injection, phosphorylated α-synuclein pathology had spread throughout the right hemisphere and the left hemisphere.

dementia with Lewy bodies brain extracts), but extracts of brains with dementia with Lewy bodies showed lower propagation efficiency than recombinant fibrils (Table 2). This relatively low efficiency may be explained by the lesser amount of abnormal α-synuclein contained in the dementia with Lewy bodies brain extracts. Comparison of human α-synuclein fibrils and mouse α-synuclein fibrils indicated that mouse α-synuclein fibrils showed slightly higher efficiency (Table 2). *In vitro* experiments also indicated that mouse α-synuclein fibrils promote fibrillization of the soluble mouse α-synuclein monomer faster than human α-synuclein fibrils (Supplementary Fig. 7). It is well known that prion propagation can cross the species barrier (Prusiner, 1993) and the efficiency of propagation depends on the amino acid sequences of prion proteins. In the case of α-synuclein, mouse α-synuclein and human α-synuclein share 95% amino acid sequence homology (Supplementary Fig. 5), and this may be the reason why endogenous mouse α-synuclein is capable of aggregation by inoculation of human α-synuclein fibrils. Another factor may be that mouse α-synuclein protein has a threonine residue at amino acid position 53 (Supplementary Fig. 5), which is known as an aggregation-prone mutation in familial Parkinson's disease (Polymeropoulos *et al.*, 1997).

Time course analyses of the pathology in these mice (Table 1) showed that at 90 days after injection, phosphorylated α-synuclein pathology was mainly observed near the injection level, but also seen in striatum, amygdala, stria terminalis and dentate gyrus: areas far from the injection site had developed pathology. The striatum and the amygdala central nucleus have projections from substantia nigra, and the stria terminalis serves as a major output pathway of the amygdala (Supplementary Fig. 8). Although the

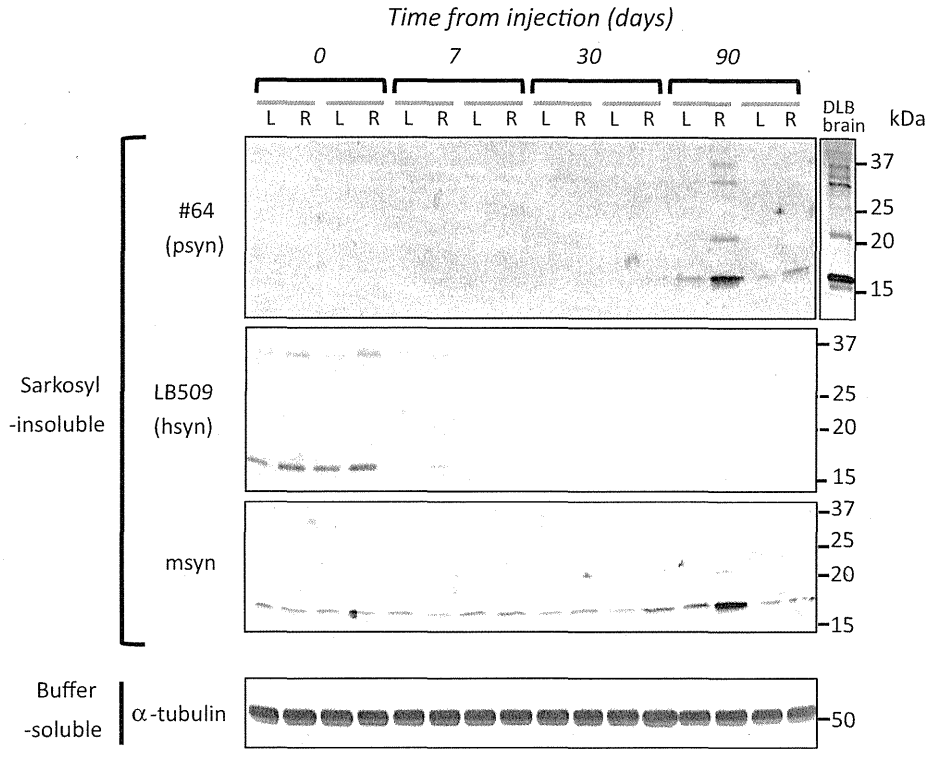

Figure 4 Endogenous mouse α-synuclein was aggregated in wild-type mouse brain injected with human α-synuclein (hsyn) fibrils. The brain was divided into two parts at the longitudinal fissure of the cerebrum. Sarkosyl-insoluble fractions were obtained from the right and left hemispheres, and analysed by immunoblotting with #64, LB509 or anti-mouse α-synuclein (msyn) antibodies. Representative images are shown (n = 14). Sarkosyl-insoluble phosphorylated α-synuclein (psyn) started to accumulate, predominantly in the right hemisphere, at 90 days after injection. It was composed of endogenous mouse α-synuclein, not exogenous human α-synuclein.

dentate gyrus does not have direct projection to substantia nigra, regions connecting with dentate gyrus (i.e., hippocampal CA1, CA3, entorhinal cortex, fimbria, fornix and hippocampal commissure) also showed moderate pathology (Table 1). These results may indicate that α-synuclein pathology propagates unidirectionally through the neural circuit (Supplementary Fig. 8). Spread of pathology from the right hemisphere to the left hemisphere might occur via the corpus callosum, hippocampal commissure, etc., connecting with the contralateral side of the brain (Fig. 3B and Table 1). Phosphorylated α-synuclein pathology in our mouse model was mainly observed in neurons and was hardly detected in glial cells, while the band pattern of sarkosyl-insoluble phosphorylated α-synuclein in mice was indistinguishable from that of dementia with Lewy bodies brains (Fig. 4), where phosphorylated α-synuclein pathology was mainly seen in neurons. Although the mechanism remains to be clarified, exogenous α-synuclein fibrils may enter cells through a selective mechanism(s), such as neuron-specific receptors. Alternatively, differences in expression levels of endogenous α-synuclein or cellular environments may also be important for formation of the pathology, even if abnormal α-synuclein has already entered the cells.

Luk *et al.* (2012*a*) reported dopaminergic neuronal loss and motor dysfunction (by Rotarod test and wire hang test) in wild-type mice injected with mouse α-synuclein fibrils at 6 months after inoculation into striatum. In contrast, our human α-synuclein or mouse α-synuclein fibril-injected mice did not

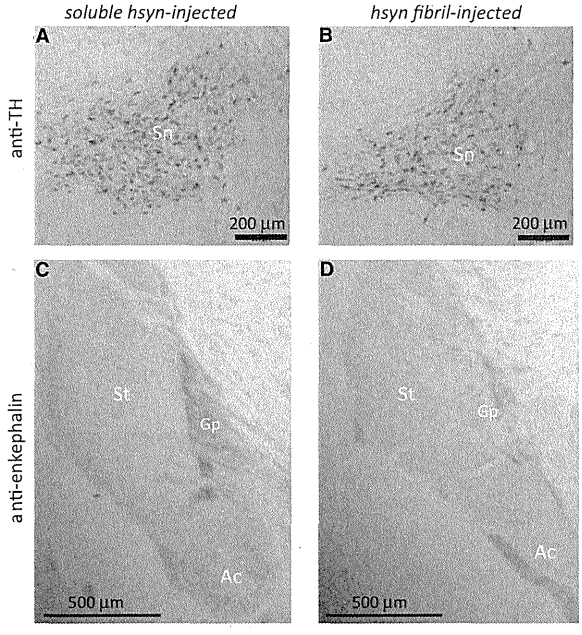

Figure 5 Fibril-injected mice show apparent reduction of a neurotransmitter enkephalin in amygdala central nucleus and globus pallidus at 15 months after injection. Brain sections were stained with anti-tyrosine hydroxylase (TH) (**A** and **B**) and anti-enkephalin (**C** and **D**) antibodies. Ac = amygdala central nucleus; Gp = globus pallidus; Sn = substantia nigra; St = striatum.

Table 2 **Comparison of propagation efficiency in mice at 15 months after injection**

Injection samples		Right hemisphere (injection side) anti-psyn	anti-ubiquitin	anti-p62	Left hemisphere (non-injected side) anti-psyn
Soluble human α-syn	(*n* = 8)	0/8 (0%)	0/8 (0%)	0/8 (0%)	0/8 (0%)
Insoluble human α-syn fibril	(*n* = 24)	22/24 (91.6%)	21/24 (87.5%)	22/24 (91.6%)	19/24 (79.2%)
Soluble mouse α-syn	(*n* = 4)	0/4 (0%)	0/4 (0%)	0/4 (0%)	0/4 (0%)
Insoluble mouse α-syn fibril	(*n* = 8)	8/8 (100%)	7/8 (87.5%)	8/8 (100%)	8/8 (100%)
DLB brain extracts	(*n* = 14)	7/14 (50%)	0/14 (0%)	5/14 (35.7%)	1/14 (7.1%)

In the right hemisphere, mice showing immunopositive structures for anti-phosphorylated α-synuclein (psyn), ubiquitin (Ub) or p62 were counted. In the left hemisphere, mice showing immunopositive structures for anti-phosphorylated α-synuclein were counted. Values show number of immunopositive mice/total mice, with percentage of immunopositive mice. DLB = dementia with Lewy bodies.

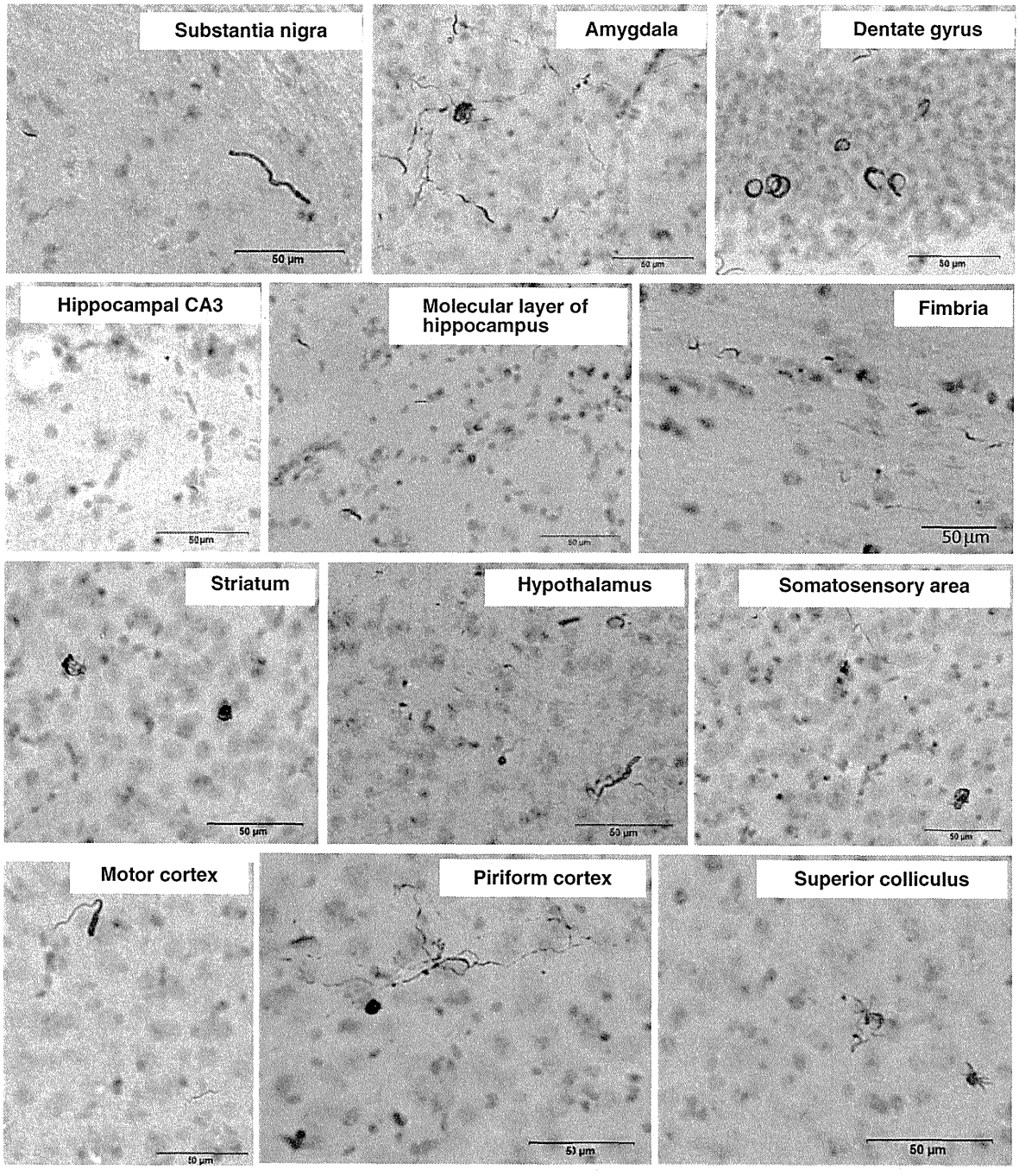

Figure 6 α-Synuclein pathology in wild-type mice brain injected with dementia with Lewy bodies-insoluble fraction observed at 15 months after injection. Sections were immunostained with anti-phosphorylated α-synuclein antibody, 1175.

show any motor and cognitive deficits at 6 months after inoculation and dopaminergic degeneration even after 15 months, a dramatic reduction of enkephalin was observed in the amygdala central nucleus and globus pallidus, with severe pathology, at 6 months after injection (Fig. 5 and Supplementary Fig. 4). The different phenotypes of these mice might be explained by differences in the injection sites [striatum in Luk *et al.* (2012*a*) and substantia nigra in our study]. Nonetheless, the spreading pattern of the pathological α-synuclein is different between our study and theirs. Differential vulnerability of neurons to these abnormal proteins may also affect phenotypes of these mice.

In summary, we have shown that intracerebral injection of insoluble α-synuclein fibrils can induce aggregation of endogenous mouse α-synuclein through a prion-like propagation mechanism. Our data suggest that phosphorylated α-synuclein pathologies do not induce acute neuronal loss but induce a slow neurodegeneration by disrupting neuronal function. These models should be useful not only for elucidating the molecular mechanisms of propagation of intracellular abnormal proteins, but also for development and evaluation of disease-modifying therapy.

Funding

This work was supported by MEXT KAKENHI Grant Numbers 12937622, 12901980 (to M.H.), JSPS KAKENHI Grant Number 11024780 (to M.M-S.) and MHLW Grant Number 12946221 (to M.H.).

Supplementary material

Supplementary material is available at *Brain* online.

References

Baba M, Nakajo S, Tu PH, Tomita T, Nakaya K, Lee VM, et al. Aggregation of alpha-synuclein in Lewy bodies of sporadic Parkinson's disease and dementia with Lewy bodies. Am J Pathol 1998; 152: 879–84.

Braak H, Braak E. Neuropathological stageing of Alzheimer-related changes. Acta Neuropathol 1991; 82: 239–59.

Chartier-Harlin MC, Kachergus J, Roumier C, Mouroux V, Douay X, Lincoln S, et al. Alpha-synuclein locus duplication as a cause of familial Parkinson's disease. Lancet 2004; 364: 1167–9.

Clavaguera F, Bolmont T, Crowther RA, Abramowski D, Frank S, Probst A, et al. Transmission and spreading of tauopathy in transgenic mouse brain. Nat Cell Biol 2009; 11: 909–13.

Desplats P, Lee HJ, Bae EJ, Patrick C, Rockenstein E, Crews L, et al. Inclusion formation and neuronal cell death through neuron-to-neuron transmission of alpha-synuclein. Proc Natl Acad Sci USA 2009; 106: 13010–5.

Emmanouilidou E, Melachroinou K, Roumeliotis T, Garbis SD, Ntzouni M, Margaritis LH, et al. Cell-produced alpha-synuclein is secreted in a calcium-dependent manner by exosomes and impacts neuronal survival. J Neurosci 2010; 30: 6838–51.

Fujiwara H, Hasegawa M, Dohmae N, Kawashima A, Masliah E, Goldberg MS, et al. Alpha-Synuclein is phosphorylated in synucleinopathy lesions. Nat Cell Biol 2002; 4: 160–4.

Goedert M. Alpha-synuclein and neurodegenerative diseases. Nat Rev Neurosci 2001; 2: 492–501.

Ibanez P, Bonnet AM, Debarges B, Lohmann E, Tison F, Pollak P, et al. Causal relation between alpha-synuclein gene duplication and familial Parkinson's disease. Lancet 2004; 364: 1169–71.

Kordower JH, Chu Y, Hauser RA, Freeman TB, Olanow CW. Lewy body-like pathology in long-term embryonic nigral transplants in Parkinson's disease. Nat Med 2008; 14: 504–6.

Kruger R, Kuhn W, Muller T, Woitalla D, Graeber M, Kosel S, et al. Ala30Pro mutation in the gene encoding alpha-synuclein in Parkinson's disease. Nat Genet 1998; 18: 106–8.

Kuusisto E, Salminen A, Alafuzoff I. Ubiquitin-binding protein p62 is present in neuronal and glial inclusions in human tauopathies and synucleinopathies. Neuroreport 2001; 12: 2085–90.

Li JY, Englund E, Holton JL, Soulet D, Hagell P, Lees AJ, et al. Lewy bodies in grafted neurons in subjects with Parkinson's disease suggest host-to-graft disease propagation. Nat Med 2008; 14: 501–3.

Luk KC, Kehm V, Carroll J, Zhang B, O'Brien P, Trojanowski JQ, et al. Pathological alpha-synuclein transmission initiates Parkinson-like neurodegeneration in nontransgenic mice. Science 2012a; 338: 949–53.

Luk KC, Kehm VM, Zhang B, O'Brien P, Trojanowski JQ, Lee VM. Intracerebral inoculation of pathological alpha-synuclein initiates a rapidly progressive neurodegenerative alpha-synucleinopathy in mice. J Exp Med 2012b; 209: 975–86.

Masuda M, Dohmae N, Nonaka T, Oikawa T, Hisanaga S, Goedert M, et al. Cysteine misincorporation in bacterially expressed human alpha-synuclein. FEBS Lett 2006a; 580: 1775–9.

Masuda M, Suzuki N, Taniguchi S, Oikawa T, Nonaka T, Iwatsubo T, et al. Small molecule inhibitors of alpha-synuclein filament assembly. Biochemistry 2006b; 45: 6085–94.

Mougenot AL, Nicot S, Bencsik A, Morignat E, Verchere J, Lakhdar L, et al. Prion-like acceleration of a synucleinopathy in a transgenic mouse model. Neurobiol Aging 2012; 33: 2225–8.

Muller CM, de Vos RA, Maurage CA, Thal DR, Tolnay M, Braak H. Staging of sporadic Parkinson disease-related alpha-synuclein pathology: inter- and intra-rater reliability. J Neuropathol Exp Neurol 2005; 64: 623–8.

Nonaka T, Kametani F, Arai T, Akiyama H, Hasegawa M. Truncation and pathogenic mutations facilitate the formation of intracellular aggregates of TDP-43. Hum Mol Genet 2009; 18: 3353–64.

Nonaka T, Watanabe ST, Iwatsubo T, Hasegawa M. Seeded aggregation and toxicity of {alpha}-synuclein and tau: cellular models of neurodegenerative diseases. J Biol Chem 2010; 285: 34885–98.

Polymeropoulos MH, Lavedan C, Leroy E, Ide SE, Dehejia A, Dutra A, et al. Mutation in the alpha-synuclein gene identified in families with Parkinson's disease. Science 1997; 276: 2045–7.

Prusiner SB. Genetic and infectious prion diseases. Arch Neurol 1993; 50: 1129–53.

Serpell LC, Berriman J, Jakes R, Goedert M, Crowther RA. Fiber diffraction of synthetic alpha-synuclein filaments shows amyloid-like cross-beta conformation. Proc Natl Acad Sci USA 2000; 97: 4897–902.

Shiotsuki H, Yoshimi K, Shimo Y, Funayama M, Takamatsu Y, Ikeda K, et al. A rotarod test for evaluation of motor skill learning. J Neurosci Methods 2010; 189: 180–5.

Singleton AB, Farrer M, Johnson J, Singleton A, Hague S, Kachergus J, et al. alpha-Synuclein locus triplication causes Parkinson's disease. Science 2003; 302: 841.

Spillantini MG, Crowther RA, Jakes R, Hasegawa M, Goedert M. alpha-Synuclein in filamentous inclusions of Lewy bodies from Parkinson's disease and dementia with lewy bodies. Proc Natl Acad Sci USA 1998; 95: 6469–73.

Spillantini MG, Schmidt ML, Lee VM, Trojanowski JQ, Jakes R, Goedert M. Alpha-synuclein in Lewy bodies. Nature 1997; 388: 839–40.

Stohr J, Watts JC, Mensinger ZL, Oehler A, Grillo SK, Dearmond SJ, et al. Purified and synthetic Alzheimer's amyloid beta (Abeta) prions. Proc Natl Acad Sci USA 2012; 109: 11025–30.

Volpicelli-Daley LA, Luk KC, Patel TP, Tanik SA, Riddle DM, Stieber A, et al. Exogenous alpha-synuclein fibrils induce Lewy body pathology leading to synaptic dysfunction and neuron death. Neuron 2011; 72: 57–71.

Wakabayashi K, Yoshimoto M, Tsuji S, Takahashi H. Alpha-synuclein immunoreactivity in glial cytoplasmic inclusions in multiple system atrophy. Neurosci Lett 1998; 249: 180–2.

Yonetani M, Nonaka T, Masuda M, Inukai Y, Oikawa T, Hisanaga S, et al. Conversion of wild-type alpha-synuclein into mutant-type fibrils and its propagation in the presence of A30P mutant. J Biol Chem 2009; 284: 7940–50.

Zarranz JJ, Alegre J, Gomez-Esteban JC, Lezcano E, Ros R, Ampuero I, et al. The new mutation, E46K, of alpha-synuclein causes Parkinson and Lewy body dementia. Ann Neurol 2004; 55: 164–73.

OPEN ACCESS Freely available online

PLOS | ONE

Methylene Blue Reduced Abnormal Tau Accumulation in P301L Tau Transgenic Mice

Masato Hosokawa[1], Tetsuaki Arai[1,2], Masami Masuda-Suzukake[3], Takashi Nonaka[3], Makiko Yamashita[3], Haruhiko Akiyama[1]*, Masato Hasegawa[3]

1 Department of Dementia and Higher Brain Function, Tokyo Metropolitan Institute of Medical Science, Tokyo, Japan, **2** Department of Psychiatry, Graduate School of Comprehensive Human Sciences, University of Tsukuba, Tsukuba, Japan, **3** Department of Pathology and Cell Biology, Tokyo Metropolitan Institute of Medical Science, Tokyo, Japan

Abstract

In neurodegenerative disorders, abnormally hyperphosphorylated and aggregated tau accumulates intracellularly, a mechanism which is thought to induce neuronal cell death. Methylene blue, a type of phenothiazine, has been reported to inhibit tau aggregation in vitro. However, the effect of methylene blue in vivo has remained unknown. Therefore, we examined whether methylene blue suppresses abnormal tau accumulation using P301L tau transgenic mice. At 8 to 11 months of age, these mice were orally administered methylene blue for 5 months. Subsequent results of Western blotting analysis revealed that this agent reduced detergent-insoluble phospho-tau. Methylene blue may have potential as a drug candidate for the treatment of tauopathy.

Citation: Hosokawa M, Arai T, Masuda-Suzukake M, Nonaka T, Yamashita M, et al. (2012) Methylene Blue Reduced Abnormal Tau Accumulation in P301L Tau Transgenic Mice. PLoS ONE 7(12): e52389. doi:10.1371/journal.pone.0052389

Editor: Andrea C. LeBlanc, McGill University, Canada

Received June 12, 2012; **Accepted** November 14, 2012; **Published** December 20, 2012

Funding: This research was partially supported by the Japan Society for the Promotion of Science, Grants-in-Aid for Scientific Research (C), grant number 21591536 to HA and 24591738 to M. Hosokawa. The additional part of the funding of the authors' study has come from institute budget. The funders had no role in study design, data collection and analysis, decision to publish, or preparation of the manuscript.

Competing Interests: The authors have declared that no competing interests exist.

* E-mail: akiyama-hr@igakuken.or.jp

Introduction

In neurodegenerative disorders such as Alzheimer's disease, corticobasal degeneration, and supranuclear palsy, the microtubule–associated protein tau is abnormally phosphorylated and redistributed into paired helical filaments (PHFs) forming neurofibrillary tangles, a process that correlates with pyramidal cell destruction and dementia. Abnormal tau accumulation is characterized by hyperphosphorylation, conformational change and aggregation with changes in solubility.

Wischik et al. have identified a nonneuroleptic phenothiazine which reverses the proteolytic stability of protease-resistant PHFs by blocking tau-tau binding through the repeat domain [1]. Moreover, phenothiazines, including methylthioninium chloride (methylene blue (MB)), polyphenols and porphyrins, inhibited heparin-induced tau filament formation in vitro [2]. Based on these results, tau aggregation inhibitors are considered to be strong candidates for the treatment of tauopathy.

TauRx Pharmaceuticals recently announced the completion of MB phase II clinical trials. They conducted MB dosing and efficacy studies involving 321 people with mild to moderate Alzheimer's disease. Over a 50-week period, the cognitive decline of those on the drug appeared to be 81% slower than those taking a placebo. These results were presented at a conference [3] but have not been published. Currently, a large-scale phase III trial is in planning [4].

To date, there are two reports on the effect of MB on tau aggregation in vivo. In one study, MB did not alter abnormal tau phosphorylation and failed to inhibit tau-dependent neuronal cell toxicity in zebrafish [5]. The other study employed a distinct tau transgenic mouse line and mice received a 2–3-week treatment with oral MB. In this latter study, MB acted as a tau aggregation inhibitor. Although, these findings have been described in brief in a conference abstract, the details are unavailable [6].

More recently, Congdon et al. demonstrated that MB could induce autophagy in primary neurons, organotypic slice cultures and tau transgenic mice (JNPL3) [7]. They also showed a 2 week oral administration of MB attenuated the total tau levels in the absence of significant changes in sarkosyl-insoluble tau levels.

In the present study, we investigated whether MB could reduce abnormal tau accumulation by carrying out long-term oral administration of MB using tau transgenic mice with the P301L mutation as a tauopathy model. Our results suggested that oral intake of MB could be a potential treatment for tauopathy.

Materials and Methods

Ethics Statement

This study was carried out in strict accordance with the recommendations provided in the Guide for the Care and Use of Laboratory Animals of the Ministry of Health, Labour and Welfare of Japan and the Ministry of Education, Culture, Sports, Science and Technology of Japan. The protocol was approved by the Committee on the Ethics of Animal Experiments of the Tokyo Metropolitan Institute of Medical Science (Permit Numbers: 22–23 and 11-028). All experiments were performed under sodium pentobarbital anesthesia and every effort was made to minimize suffering.

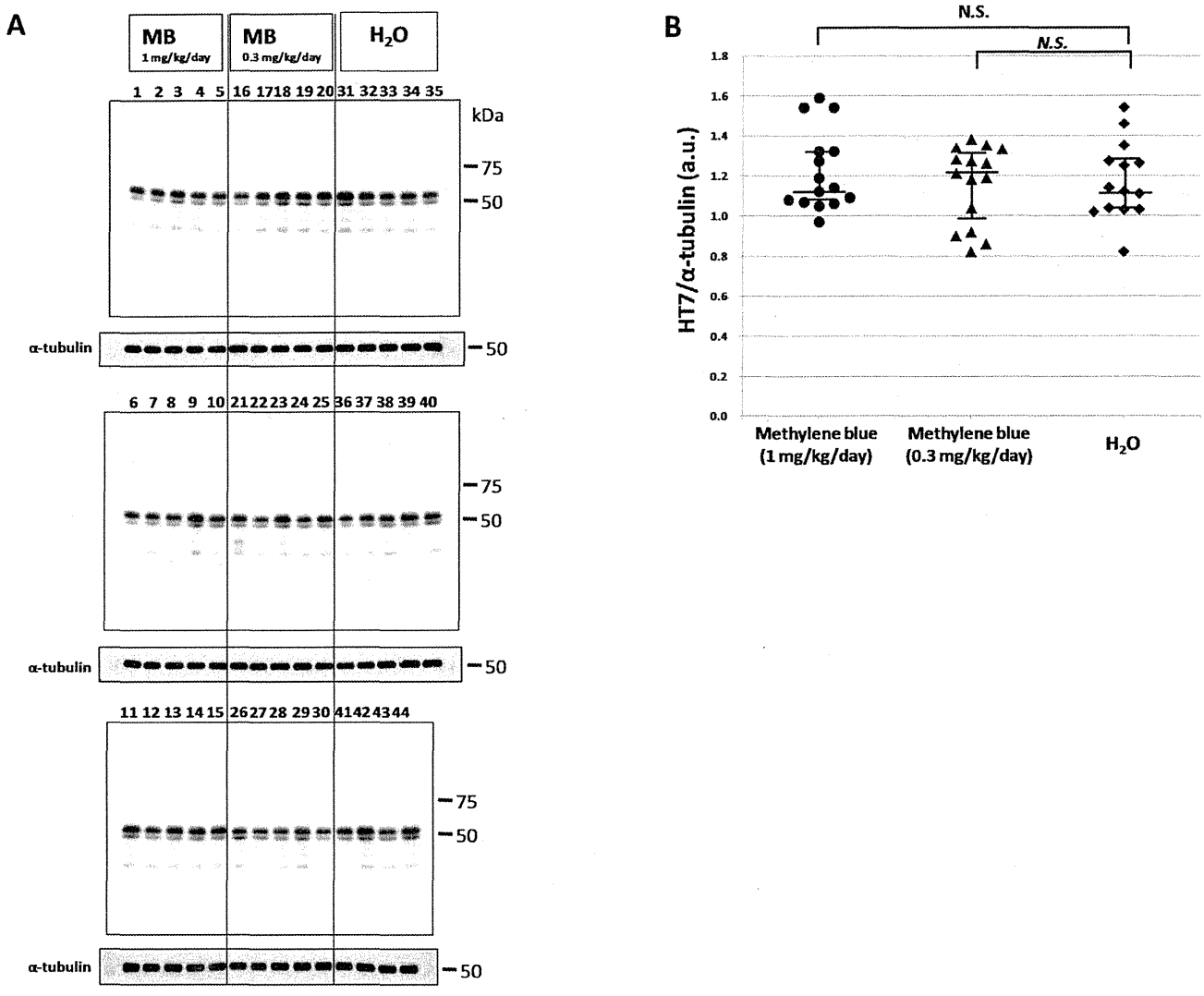

Figure 1. Immunoblotting analysis of total tau in the Tris-soluble fraction. (A) Immunoblotting analysis was visualized using HT7 antibody for the Tris-soluble fraction. The numbers indicate individual mice: 1–15, MB 1 mg/kg/day group; 16–30, MB 0.3 mg/kg/day group; and 31–44, water only group. Molecular weight markers are shown on the right (kDa). For quantitative measure of band intensity, α-tubulin was used as an internal control for protein concentration. (B) A comparison of the relative total tau (HT7) expression levels of the MB-treated groups and the water only group. The data were compared with the HT7 band intensity, which was normalized with α-tubulin. The central lines indicate medians and the vertical lines represent 25th and 75th percentiles. a.u., arbitrary unit. N.S., no significant difference.
doi:10.1371/journal.pone.0052389.g001

Animals

P301L tau transgenic mice (JNPL3) [8] were purchased from Taconic (USA) via IBL (Japan). The experiments utilized 44 female hemizygote tau mice. The mice were reared in the animal facility of Tokyo Metropolitan Institute of Medical Science under standard conditions at 24±2°C and were maintained on a commercial diet supplied ad libitum.

The transgenic mice [8] aged 8–11 months were divided into 3 groups: the first group (14 mice) was given water alone, the second group (15 mice) was given water containing 2 μg/ml MB and the third group (15 mice) was given water containing 6 μg/ml MB. All were maintained on their respective regimens for 5 months. The daily MB intake was estimated to be about 0.3 or 1 mg/kg/day per mouse, on the assumption that a mouse weighs 30 g and takes in 5 ml of water a day.

At the end of the experimental period, mice were sacrificed under quick anesthesia with 200 mg/kg body weight of sodium pentobarbital delivered intraperitoneally and their brains were quickly removed. Brains of each group were cut along the sagittal plane and the left hemisphere was frozen and stored at −80°C for biochemical analyses. The right hemisphere was fixed in 4% paraformaldehyde in 0.1 M phosphate buffer for 48 hours in the cold. Brain blocks were then transferred to a maintenance solution of 15% sucrose in 0.01 M phosphate-buffered saline (PBS), pH 7.4.

Analysis of Tau Deposition

Deposition of tau was analyzed using immunohistochemical staining with AT8 antibody (recognizes phosphorylation at both serine 202 and threonine 205) and MC-1 antibody. Biotinylation of MC-1 antibody was performed using a Zenon Mouse IgG

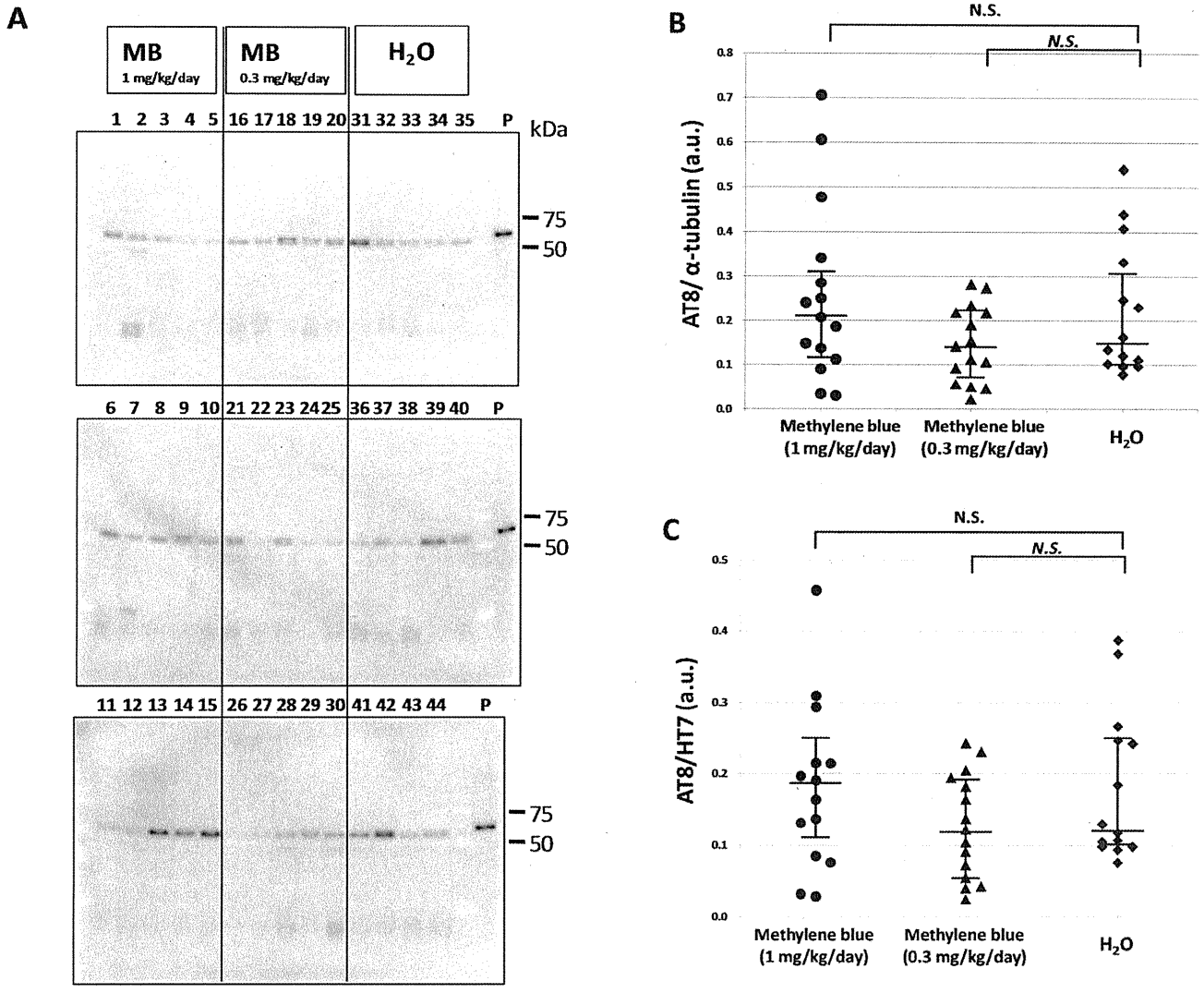

Figure 2. Immunoblotting analysis of phosphorylated tau in the Tris-soluble fraction. (A) Immunoblot analysis was visualized using AT8 antibody for the Tris-soluble fraction. The numbers indicate individual mice: 1–15, MB 1 mg/kg/day group; 16–30, MB 0.3 mg/kg/day group; and 31–44, water only group. Molecular weight markers are shown on the right (kDa). P, positive control (P301L tau transgenic mouse, 20 month-old female). (B) A comparison of relative phosphorylated tau (AT8) expression levels of the MB-treated groups and the water only group. The data were compared with the AT8 band intensity, which was normalized with α-tubulin. (C) A comparison of the relative phosphorylated tau (AT8)/total tau (HT7) levels of the MB-treated groups and the water only group. The data were compared with the AT8 band intensity, which was normalized with the total tau (HT7) band intensity. The central lines indicate medians and the vertical lines represent 25th and 75th percentiles. a.u., arbitrary unit. N.S., no significant difference.

doi:10.1371/journal.pone.0052389.g002

Labeling Kit (Molecular Probes, Inc. Eugene, OR, USA) according to the manufacturer's instructions. For immunohistochemistry, sagittal sections were cut serially on a freezing microtome at 30 μm thickness, collected in the maintenance solution, and immunostained as free-floating sections. Following a pretreatment with 0.5% H_2O_2 for 30 min to eliminate endogenous peroxidase activity, sections were incubated for 72 hours with AT8 antibody (Biotinylated-AT8, 1:1,000, Innogenetics, Ghent, Belgium) or overnight with biotinylated MC-1 antibody (1:100, a generous gift of Dr. Davies) [9] diluted in PBS containing 0.3% Triton X-100 (PBS-Tx). The antibody labeling was visualized by incubation with avidin-biotinylated horseradish peroxidase (HRP) complex (ABC Elite, 1:1,000, Vector Laboratories, Burlingame, CA, USA) for 3 hours, followed by incubation with a solution containing 0.01% 3,3′-diaminobenzidine (DAB), 1% nickel ammonium sulfate, 0.05 M imidazole and 0.00015% H_2O_2 in 0.05 M Tris-HCl buffer, pH 7.6. Counter nuclear staining was performed with Kernechtrot stain solution (Merck, Darmstadt, Germany). The sections were then rinsed with distilled water, mounted on glass slides, treated with Xylene, and coverslipped with Entellan (Merck). Photographs were taken with an Olympus VS120-S5 (Olympus, Tokyo, Japan) or a BX51 microscope (Olympus).

Sequential Fractionation of Brain Extracts

Frozen left hemispheres (approximately, 0.2 g) were homogenized in 10 volumes of buffer H (10 mM Tris-HCl, pH 7.5, 0.8 M NaCl, 1 mM ethylene glycol bis-N, N, N', N'-tetraacetic acid, 1 mM dithiothreitol). The hemisphere included the olfactory bulb, cerebral cortex, striatum, thalamus, hypothalamus, cerebellum,

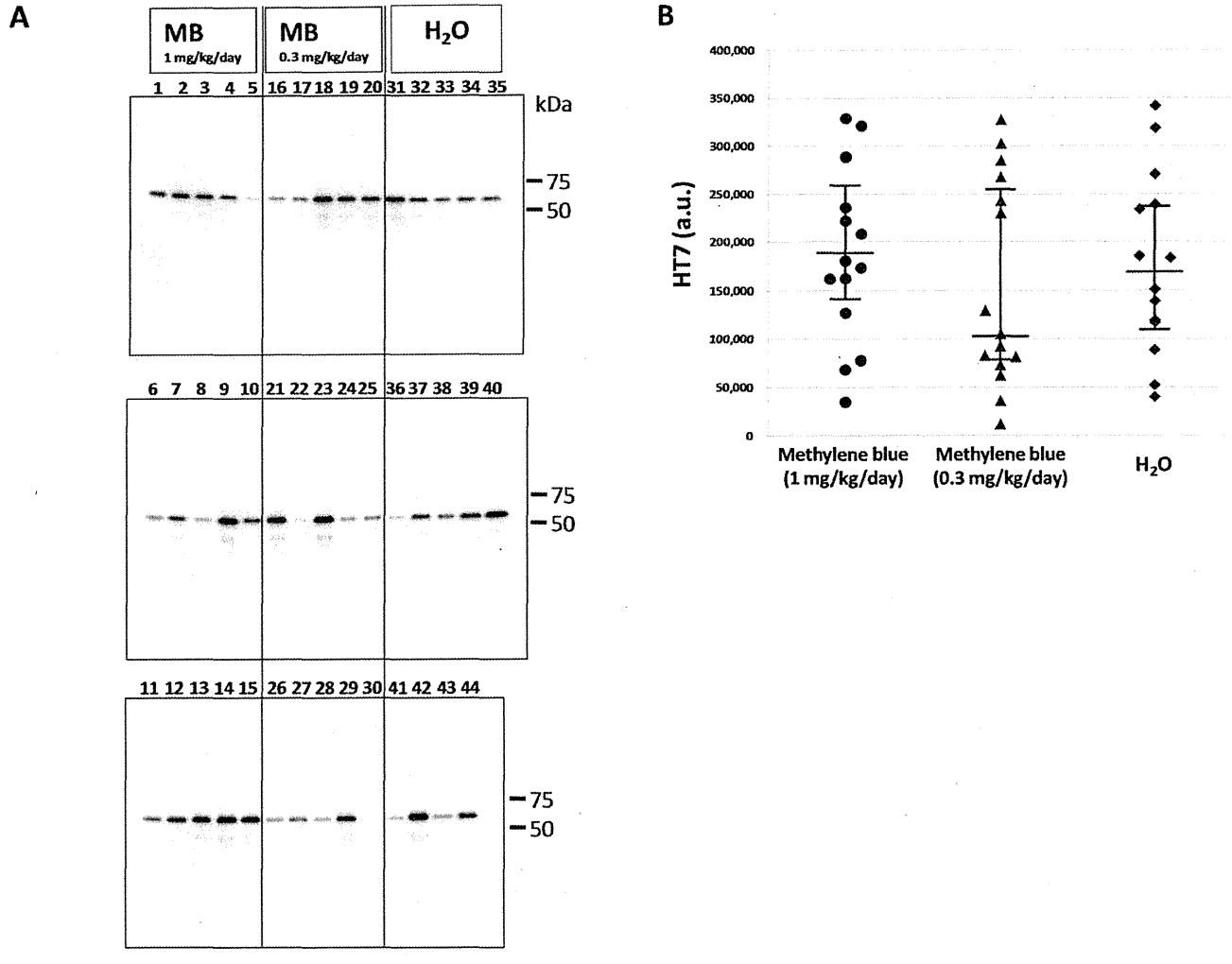

Figure 3. Immunoblotting analysis of total tau in the sarkosyl-insoluble fraction. (A) Immunoblot analysis was visualized using HT7 antibody for the sarkosyl-insoluble fraction. The numbers indicate individual mice: 1–15, MB 1 mg/kg/day group; 16–30, MB 0.3 mg/kg/day group; 31–44, water only group. Molecular weight markers are shown on the right (kDa). (B) A comparison of relative total tau (HT7) expression levels in the sarkosyl-insoluble fraction of the MB-treated groups and the water only group. The data were compared with the HT7 band intensity. The central lines indicate medians and the vertical lines represent 25th and 75th percentiles. a.u., arbitrary unit.
doi:10.1371/journal.pone.0052389.g003

midbrain, pons, medulla oblongata and the upper part of the spinal cord. The method used for sequential fractionation of brain extracts was originally described by Greenberg et al. [10]. Briefly, the brain homogenate was centrifuged at 100,000×g for 20 min at 4°C, and the supernatants were collected as the Tris-soluble fraction. The resultant pellet was homogenized in 10 volumes of buffer H, followed by an incubation for 30 min at 37°C with 1% Triton X-100. The homogenate was then centrifuged at 100,000×g for 20 min at 4°C. The Triton X-100 insoluble pellet was sonicated in 5 volumes of buffer H containing 1% sarkosyl and centrifuged at 100,000×g for 20 min at 4°C. The pellet was then sonicated in 1 volume of SDS-PAGE sample buffer.

Immunoblotting Analysis

For immunoblotting, brain extracts from the tau mice were boiled for 5 minutes with SDS-PAGE sample buffer (60 mM Tris-HCl, pH 6.8, containing 2% SDS, 10% glycerol, 0.025% bromophenol blue and 5% mercaptoethanol) and loaded onto a 10% acrylamide minigel. Loaded samples were electrophoresed for 45 minutes at 200 V with molecular weight markers (Bio-Rad, Hercules, CA, USA). Electrophoresed proteins were transferred onto a polyvinylidene difluoride membrane (Millipore, Billerica, MA, USA) for 60 minutes at 200 mA. The printed membranes were blocked with 3% gelatin for 1 hour and then incubated in a primary antibody solution (HT7, 1:3,000, Innogenetics, AT8, 1:3,000, Innogenetics, or anti-α-tubulin, 1:10,000, Sigma, St. Louis, MO, USA) overnight at room temperature. Following incubation with a secondary antibody (1:20,000, Bio-Rad), immunoreactivity was detected by the chemiluminescence method using an ECL plus Western Blotting Detection Kit (GE Healthcare UK Ltd., Buckinghamshire, England) or SuperSignal West Dura Extended Duration Substrate (Pierce, Rockford IL, USA) and was visualized with LAS-3000 (Fujifilm, Tokyo, Japan). For quantitative measure of band intensity, α-tubulin was used as an internal control for protein concentration.

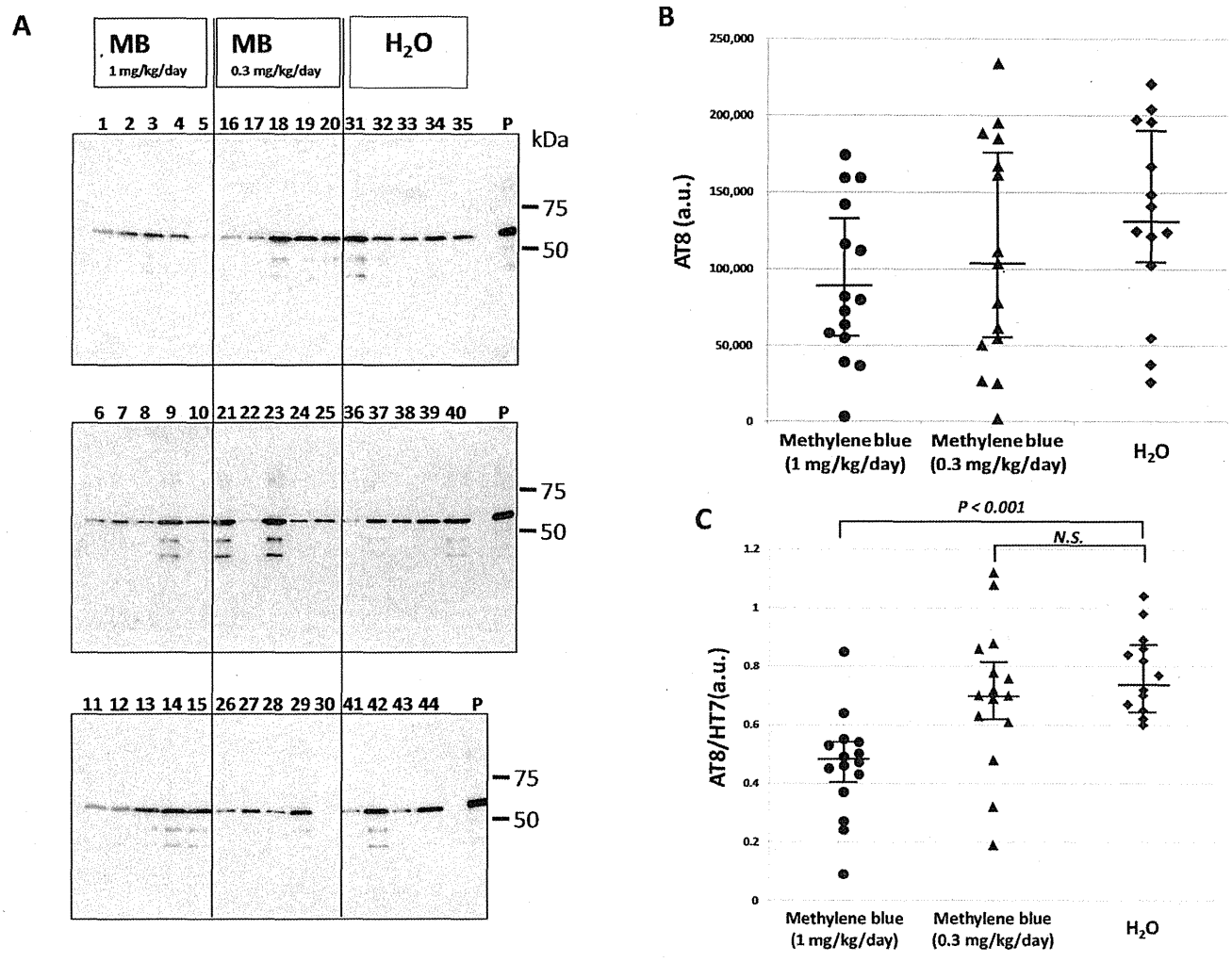

Figure 4. Immunoblotting analysis of abnormal tau in the sarkosyl-insoluble fraction. (A) Immunoblotting analysis was visualized using AT8 antibody for the sarkosyl-insoluble fraction. The numbers indicate individual mice: 1–15, MB 1 mg/kg/day group; 16–30, MB 0.3 mg/kg/day group; and 31–44, water only group. Molecular weight markers are shown on the right (kDa). P, positive control (P301L tau transgenic mouse, 20 month-old female). (B) A comparison of relative AT8 expression levels of the MB-treated groups and the water only group. The data were compared with the AT8 band intensity. (C) A comparison of relative phosphorylated tau (AT8)/total tau (HT7) levels of the MB-treated groups and the water only group. The data were compared with the AT8 band intensity, which was normalized with the total tau (HT7) band intensity. The central lines indicate medians and the vertical lines represent 25th and 75th percentiles. $P<0.01$ was considered to represent a statistically significant difference. a.u., arbitrary unit. N.S., no significant difference.
doi:10.1371/journal.pone.0052389.g004

Statistical Analyses

The data are presented as medians (interquartile range) [range]. The significance of difference between values was estimated by means of Kruskal-Wallis analysis of variances with post hoc Steel's method. $P<0.05$ was considered to indicate a statistically significant difference.

Results

Immunoblotting Analysis

To investigate the effect of methylene bule on tau accumulation, P301L tau transgenic mice were administered MB for 5 months starting at 8–11 months of age. Brains were then collected and sequential protein extraction and immunoblotting were performed (Figs. 1, 2, 3, 4). Total tau in the Tris-soluble fraction was detected by HT7 antibody (Fig. 1A), and there were no prominent differences among the three groups by quantitative analysis of band intensities, which was normalized with α-tubulin (Fig. 1B). Phosphorylated tau in the Tris-soluble fraction was also detected by AT8 antibody (Fig. 2A). The data were compared with the AT8 band intensity, which was normalized with α-tubulin (Fig. 2B) or with the total tau (HT7) band intensity (Fig. 2C). There were also no significant differences in phosphorylated tau in the Tris-soluble fraction among the three groups (Figs. 2B and 2C).

Phosphorylated tau and total tau in the sarkosyl-insoluble fraction were visualized again by Western blotting using HT7 antibody (Fig. 3A) and AT8 (Fig. 4A), respectively. The HT7 (Fig. 3B) and AT8 (Fig. 4B) band intensities were measured. Then, we compared the AT8 band intensity normalized by the total tau (HT7) band intensity and were expressed as medians (interquartile range) [range]. The AT8/HT7 ratio was 0.47 (0.40–0.53) [0.09–0.85] (n = 15) in the MB group given 1 mg/kg/day, 0.70 (0.62–0.82) [0.19–1.12] (n = 15) in the MB group given 0.3 mg/kg/day, and 0.74 (0.65–0.86) [0.60–1.04] (n = 14) in the group given water

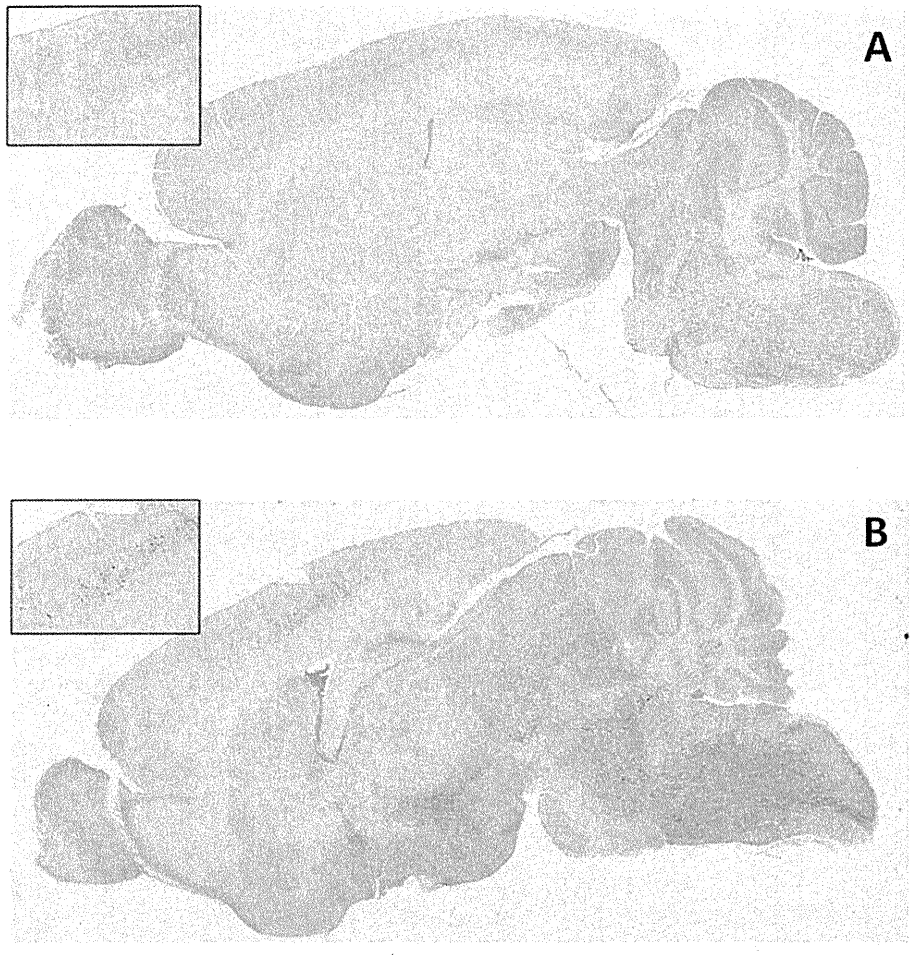

Figure 5. Immunohistochemical staining of abnormal tau. (A) An AT8 immunoreaction was observed only in spinal cord, medulla oblongata and pons of a mouse with a low AT8/HT7 ratio. (B) AT8-positive cells were seen in spinal cord, medulla oblongata, pons, midbrain, hypothalamus and cerebral cortex of a mouse with a high AT8/HT7 ratio. Each insert shows the cerebral cortex of the mouse brain.
doi:10.1371/journal.pone.0052389.g005

alone (Fig. 4C). The Kruskal-Wallis test followed by Steel's multiple comparison test was used for statistical analyses, and there was a significant difference between the group given MB 1 mg/kg/day and the group given water alone ($P<0.001$). There was no significant difference between the 0.3 mg/kg/day group and the water only group ($P = 0.422$). Immunoblotting analysis revealed that the level of abnormally phosphorylated tau accumulation was decreased in the P301L tau mice given MB as compared with the P301L tau mice given water alone.

Analysis of Tau Deposition

A weak AT8 immunoreaction was observed only in the spinal cord, medulla oblongata and pons of the mice with a low AT8/HT7 ratio (Fig. 5A). On the other hand, AT8-positive cells were seen in the spinal cord, medulla oblongata, cerebellar nuclei, pons, midbrain, hypothalamus and primary motor cortex of mice with a high AT8/HT7 ratio (Fig. 5B). Immunohistochemical staining with a conformational antibody, MC-1, which recognizes aggregated tau showed that MC-1-positive neurons and cellular processes were seen in the motor cortex, hypothalamus and pons (Fig. 6). However, MC-1-positive neurons and cellular processes in these areas of mice with a low AT8/HT7 ratio were significantly fewer than those in mice with a high AT8/HT7 ratio.

Discussion

Cases of dementia including AD have been increasing in number in recent years, and discovering effective drugs for treating these diseases must be facilitated. Developing a novel drug for the treatment of AD is a time-consuming process and a better approach might be through screening chemical compounds or drugs which are already available. Consequently, we evaluated MB inhibition of abnormal tau accumulation using a tauopathy mouse model, since MB had been shown to be a protein aggregation inhibitor *in vitro* [2] as well as more recently in cells [11].

MB was found to have an inhibitory effect on tau aggregation *in vitro* [1–2] and to act as a tau aggregation inhibitor in a cellular model as well as in transgenic mice [6]. However, in the latter case, only an abstract was published on these findings and the details were unavailable. More recently, Congdon et al. reported that MB induced autophagy and attenuated tauopathy in vitro and in vivo [7]. They administrated MB (0.02, 2, and 20 mg/kg) to tau transgenic mice (JNPL3) by oral gavage 5 days a week for 2 weeks and performed immunoblotting for total human tau and sarkosyl-insoluble fractions. There was a significant reduction in the levels of total tau and phosphorylated tau in their MB-treated mice, however, the levels of sarkosyl-insoluble tau were unchanged

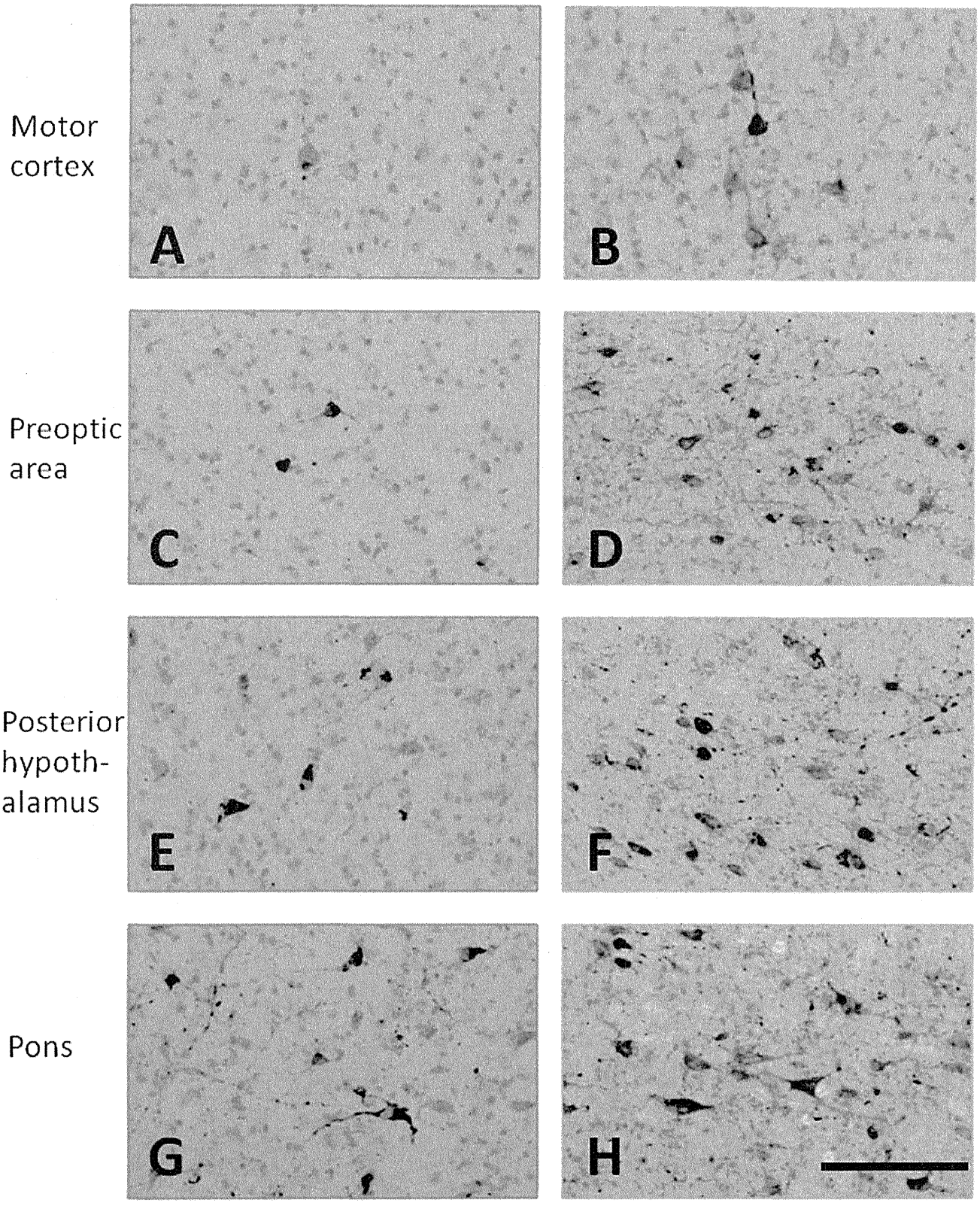

Figure 6. Immunohistochemical staining with a conformational antibody that recognizes aggregated tau. MC-1-positive neurons and cellular processes were seen in the motor cortex (A and B), prepotic area (C and D), posterior hypothalamus (E and F) and pons (G and H). A, C, E, G, mouse with a low AT8/HT7 ratio; and B, D, F, H, mouse with a high AT8/HT7 ratio. The calibration bar in H applies to all photomicrographs (50 μm).
doi:10.1371/journal.pone.0052389.g006

[7]. In the present study, the immunoblotting data revealed that phosphorylated tau was decreased in the sarkosyl-insoluble fraction after MB administration (Fig. 4). In both soluble and insoluble fractions, the amount of total tau did not differ among the three groups (Fig. 1 and 3), suggesting that the MB administration did not affect the transgenic tau expression but reduced the aggregation of phosphorylated tau. Moreover, immunohistochemical staining demonstrated that MB inhibited the spread of abnormal tau deposition from the brain stem to the cerebral cortex (Fig. 5 and 6). These immunohistochemistry findings supported the results obtained by immunoblotting.

The results of this study may agree with those by Congdon et al. in that the MB treatment reduced phosphorylated tau levels [7]. They also found reduction in the total tau levels in the total but not sarkosyl-insoluble brain fractions. While we did not examine the total brain fractions, we did not see significant changes in the levels of both soluble and insoluble tau between the MB and water treated groups. The reason for such a difference remains unknown, but it might be noteworthy that the duration of MB treatments was quite different between the two studies; we administrated MB 7 days a week for 5 months whereas they did 5 days a week for 2 weeks.

In a study by Medina et al., 0.025% MB was supplied in food to 3×Tg AD mice from 6 to 10 months of age. These mice subsequently showed reduced Aβ levels (soluble $A\beta_{40}$ and $A\beta_{42}$) and were rescued from an early cognitive deficit by an increase in proteasome activity [12]. MB improved learning and memory in these mice and the MB treatment did not affect mitochondrial function or tau pathology. In contrast, Necula et al. demonstrated that MB inhibited Aβ oligomerization by promoting fibril formation in vivo [13].

MB did not affect abnormal tau phosphorylation in a tau transgenic zebrafish model [5]. It also failed to inhibit tau and polyglutamine-protein-dependent toxicity in zebrafish, although polyglutamine aggregation was dramatically reduced. These negative results led to the conclusion that an insufficient dose of MB had been used in vivo [5]. Fertilized eggs of tau transgenic fish were cultured in a buffer containing 10^{-5}% MB. However, this transgenic model was not suitable for in vivo analysis of protein aggregation and deposition. Recently, Yamashita et al. reported that MB prevented deposition of TDP-43 in a cell culture model based on ectopic overexpression of TDP-43 [11]. These findings suggested that MB would have an anti-aggregation effect on other neurodegeneration-associated proteins.

Recent reports have indicated that MB affects the brain in many ways: it inhibits butyrylcholinesterase activity [14], inhibits noradrenalin re-uptake [15], reduces cGMP and nitric oxide [16], increases extracellular levels of serotonin (5-HT) in rat brain [12], and modulates the functions of AMPA/kainate and NMDA-type ionotropic glutamate receptors [17–18]. The beneficial effect on cognitive function observed in AD patients after MB administration may be in part attributable to its influence on the cholinergic, serotonergic and glutamatergic systems [3]. MB also improves mitochondrial respiration by shuttling electrons to oxygen in the electron transport chain, and corrects perturbations in mitochondrial metabolism induced by mutagens [19–20].

Our study suggests that MB has disease-modifying activity in targeting tauopathy involving AD. The administration of MB carried out here was very simple and could easily be applied in screening other compounds for targeting tauopathy. MB could be a leading candidate, and some MB derivatives might be exploited to develop even stronger inhibition of tau aggregation.

MB has already been used for the treatment of methemoglobinemia [21–22], septic shock [23–24], and Plasmodium infection (malaria) [25–26], which may expedite its quick approval as a potential therapeutic agent for tauopathy. While the mechanism involved remains unknown, our data suggest that administration of methylene blue might reduce abnormal tau accumulation. Finally, we did not study pharmacokinetics of MB. Congdon et al. [7] demonstrated the brain concentration of MB increased in parallel with the given doses, but this is an issue that also needs futher, more detailed exploration.

Acknowledgments

We thank Dr. P. Davies for providing MC-1 antibody. We thank Ms. Hiromi Kondo for immunohistochemical staining and Ms. Erika Arakawa for technical assistance and animal care. We also thank Dr. William Campbell and Catherine Campbell for editing of the manuscript.

Author Contributions

Conceived and designed the experiments: M. Hosokawa TA HA. Performed the experiments: M. Hosokawa MM-S. Analyzed the data: M. Hosokawa MM-S TN MY HA M. Hasegawa. Contributed reagents/materials/analysis tools: MM-S TN M. Hasegawa. Wrote the paper: M. Hosokawa TA HA.

References

1. Wischik CM, Edwards PC, Lai RY, Roth M, Harrington CR (1996) Selective inhibition of Alzheimer disease-like tau aggregation by phenothiazines. Proc Natl Acad Sci U S A 93: 11213–11218.
2. Taniguchi S, Suzuki N, Masuda M, Hisanaga S, Iwatsubo T, et al. (2005) Inhibition of heparin-induced tau filament formation by phenothiazines, polyphenols, and porphyrins. J Biol Chem 280: 7614–7623.
3. Wischik CM, Bentham P, Wischik DJ, Seng KM (2008) Tau aggregation inhibitor (TAI) therapy with Rember arrests disease progression in mild and moderate Alzheimer's disease over 50 weeks. Alzheimer's & Dementia 8: T167.
4. Gravitz L (2011) Drugs: a tangled web of targets. Nature 475: S9–11.
5. van Bebber F, Paquet D, Hruscha A, Schmid B, Haass C (2010) Methylene blue fails to inhibit Tau and polyglutamine protein dependent toxicity in zebrafish. Neurobiol Dis 39: 265–271.
6. Harrington C, Rickard JE, Horsley D, Harrington KA, Hindley KP, et al. (2008) Methylthioninium chloride (MTC) acts as a tau aggregation inhibitor (TAI) in a cellular model and reverses tau pathology in transgenic mouse models of Alzheimer's disease. Alzheimer's & Dementia 4: T120–T121.
7. Congdon EE, Wu JW, Myeku N, Figueroa YH, Herman M, et al. (2012) Methylthioninium chloride (methylene blue) induces autophagy and attenuates tauopathy in vitro and in vivo. Autophagy 8: 609–622.
8. Lewis J, McGowan E, Rockwood J, Melrose H, Nacharaju P, et al. (2000) Neurofibrillary tangles, amyotrophy and progressive motor disturbance in mice expressing mutant (P301L) tau protein. Nat Genet 25: 402–405.
9. Wolozin B, Davies P (1987) Alzheimer-related neuronal protein A68: specificity and distribution. Ann Neurol 22: 521–526.
10. Greenberg SG, Davies P (1990) A preparation of Alzheimer paired helical filaments that displays distinct tau proteins by polyacrylamide gel electrophoresis. Proc Natl Acad Sci U S A 87: 5827–5831.
11. Yamashita M, Nonaka T, Arai T, Kametani F, Buchman VL, et al. (2009) Methylene blue and dimebon inhibit aggregation of TDP-43 in cellular models. FEBS Lett 583: 2419–2424.
12. Medina DX, Caccamo A, Oddo S (2011) Methylene blue reduces abeta levels and rescues early cognitive deficit by increasing proteasome activity. Brain Pathol 21: 140–149.
13. Necula M, Breydo L, Milton S, Kayed R, van der Veer WE, et al. (2007) Methylene blue inhibits amyloid Abeta oligomerization by promoting fibrillization. Biochemistry 46: 8850–8860.
14. Kucukkilinc T, Ozer I (2007) Multi-site inhibition of human plasma cholinesterase by cationic phenoxazine and phenothiazine dyes. Arch Biochem Biophys 461: 294–298.
15. Chies AB, Custodio RC, de Souza GL, Correa FM, Pereira OC (2003) Pharmacological evidence that methylene blue inhibits noradrenaline neuronal uptake in the rat vas deferens. Pol J Pharmacol 55: 573–579.
16. Heiberg IL, Wegener G, Rosenberg R (2002) Reduction of cGMP and nitric oxide has antidepressant-like effects in the forced swimming test in rats. Behav Brain Res 134: 479–484.

17. Gonzalez-Lima F, Bruchey AK (2004) Extinction memory improvement by the metabolic enhancer methylene blue. Learn Mem 11: 633–640.
18. Wrubel KM, Riha PD, Maldonado MA, McCollum D, Gonzalez-Lima F (2007) The brain metabolic enhancer methylene blue improves discrimination learning in rats. Pharmacol Biochem Behav 86: 712–717.
19. Visarius TM, Stucki JW, Lauterburg BH (1997) Stimulation of respiration by methylene blue in rat liver mitochondria. FEBS Lett 412: 157–160.
20. Atamna H, Nguyen A, Schultz C, Boyle K, Newberry J, et al. (2008) Methylene blue delays cellular senescence and enhances key mitochondrial biochemical pathways. FASEB J 22: 703–712.
21. Kristiansen JE (1989) Dyes, antipsychotic drugs, and antimicrobial activity. Fragments of a development, with special reference to the influence of Paul Ehrlich. Dan Med Bull 36: 178–185.
22. Mansouri A, Lurie AA (1993) Concise review: methemoglobinemia. Am J Hematol 42: 7–12.
23. Schneider F, Lutun P, Hasselmann M, Stoclet JC, Tempe JD (1992) Methylene blue increases systemic vascular resistance in human septic shock. Preliminary observations. Intensive Care Med 18: 309–311.
24. Preiser JC, Lejeune P, Roman A, Carlier E, De Backer D, et al. (1995) Methylene blue administration in septic shock: a clinical trial. Crit Care Med 23: 259–264.
25. Schirmer RH, Coulibaly B, Stich A, Scheiwein M, Merkle H, et al. (2003) Methylene blue as an antimalarial agent. Redox Rep 8: 272–275.
26. Rengelshausen J, Burhenne J, Frohlich M, Tayrouz Y, Singh SK, et al. (2004) Pharmacokinetic interaction of chloroquine and methylene blue combination against malaria. Eur J Clin Pharmacol 60: 709–715.

Acta Neuropathol (2012) 124:383–394
DOI 10.1007/s00401-012-0984-6

ORIGINAL PAPER

Localization of fused in sarcoma (FUS) protein to the post-synaptic density in the brain

Naoya Aoki · Shinji Higashi · Ito Kawakami · Zen Kobayashi · Masato Hosokawa · Omi Katsuse · Takashi Togo · Yoshio Hirayasu · Haruhiko Akiyama

Received: 26 January 2012 / Revised: 2 April 2012 / Accepted: 8 April 2012 / Published online: 18 April 2012

Abstract Mutations in the fused in sarcoma (*FUS*) gene are linked to a form of familial amyotrophic lateral sclerosis (ALS), ALS6. The FUS protein is a major component of the ubiquitin-positive neuronal cytoplasmic inclusions in both ALS6 and some rare forms of frontotemporal lobar degeneration (FTLD). The latter are now collectively referred to as FTLD-FUS. In the present study, we investigated the localization of FUS in human and mouse brains. FUS was detected by western blot as an approximately 72 kDa protein in both human and mouse brains. Immunohistochemistry using lightly fixed tissue sections of human and mouse brains revealed FUS-positive granular staining in the neuropil, in addition to nuclear staining. Such granules are abundant in the gray matter of the brainstem and spinal cord. They are not frequent in the telencephalon. At the light microscopic level, FUS-positive granules are often co-localized with synaptophysin and present in association with microtubule-associated protein 2-positive dendrites. In the synaptosomal fraction of mouse brain, FUS is detected mainly in the post-synaptic density fraction. Thus, while FUS is primarily a nuclear protein, it may also play a role in dendrites. In the brains of patients with FTLD with TDP-43 deposition (FTLD-TDP), the number of FUS-positive granules in the cortex is increased compared with control cases. The increase in Alzheimer's disease (AD) is less remarkable but still significant. The dendritic localization of FUS and its increase in FTLD-TDP and AD may have some implication for the pathophysiology of neurodegenerative diseases.

Keywords FUS · Dendrite · Synapse · TDP-43

Electronic supplementary material The online version of this article (doi:10.1007/s00401-012-0984-6) contains supplementary material, which is available to authorized users.

N. Aoki · S. Higashi · I. Kawakami · Z. Kobayashi · M. Hosokawa · H. Akiyama (✉)
Dementia Project, Department of Dementia and Higher Brain Function, Tokyo Metropolitan Institute of Medical Science, 2-1-6 Kamikitazawa, Setagaya-ku, Tokyo 156-8506, Japan
e-mail: akiyama-hr@igakuken.or.jp

N. Aoki · I. Kawakami · O. Katsuse · T. Togo · Y. Hirayasu
Department of Psychiatry, Yokohama City University School of Medicine, Yokohama, Japan

Introduction

Frontotemporal lobar degeneration (FTLD) is the second most common cause of dementia in populations below the age of 65 years [7]. FTLD is characterized by behavior and personality changes, language impairment, and cognitive decline [31, 39]. FTLD comprises three clinical subtypes: frontotemporal dementia (FTD), progressive non-fluent aphasia, and semantic dementia [31]. FTD is often accompanied by motor neuron involvement [37], in which case the patients manifest features of amyotrophic lateral sclerosis (ALS), a fatal neurodegenerative disease characterized by relentless degeneration of both upper and lower motor neurons. ALS has recently become recognized as a disease that involves multiple brain regions in addition to the motor neuron system [14]. Approximately a half of patients with ALS are now known to have evidence for cognitive impairment, behavior impairment or both [36], features that resemble FTD.

Two nuclear proteins, TAR DNA-binding protein 43 (TDP-43) and fused in sarcoma (FUS; also known as translated in liposarcoma), have emerged recently as FTLD and ALS-associated proteins. TDP-43 was identified as the major component of ubiquitinated aggregates in affected neuronal